Overexpression of budding yeast protein phosphatase Ppz1 impairs translation

Carlos Calafí[1,4,a], María López-Malo[1,a], Diego Velázquez[1,4], Chunyi Zhang[1], José Fernández-Fernández[2,3], Olga Rodríguez-Galán[2,3], Jesús de la Cruz[2,3], Joaquín Ariño[1,4], Antonio Casamayor[1,4,*]

[1] Institut de Biotecnologia i Biomedicina, Universitat Autònoma de Barcelona, Cerdanyola del Vallès, Catalonia, Spain.
[2] Instituto de Biomedicina de Sevilla, Hospital Universitario Virgen del Rocío/CSIC/Universidad de Sevilla, Seville, Spain.
[3] Departamento de Genética, Facultad de Biología, Universidad de Sevilla, Seville, Spain.
[4] Departament de Bioquímica i Biologia Molecular, Facultat de Veterinària, Universitat Autònoma de Barcelona, Cerdanyola del Vallès, Catalonia, Spain.

[a] These authors contributed equally to this work and are listed in alphabetical order.
* Correspondence to Antonio Casamayor, e-mail: antonio.casamayor@uab.cat

Keywords

Ppz1; protein phosphatase; ribosomal proteins; translation initiation; yeast.

ABSTRACT

The Ser/Thr protein phosphatase Ppz1 from *Saccharomyces cerevisiae* is the best characterized member of a family of enzymes only found in fungi. Ppz1 is regulated *in vivo* by two inhibitory subunits, Hal3 and Vhs3, which are moonlighting proteins also involved in the decarboxylation of the 4-phosphopantothenoylcysteine (PPC) intermediate required for coenzyme A biosynthesis. It has been reported that, when overexpressed, Ppz1 is the most toxic protein in yeast. However, the reasons for such toxicity have not been elucidated. Here we show that the detrimental effect of excessive Ppz1 expression is due to an increase in its phosphatase activity and not to a plausible down-titration of the PPC decarboxylase components. We have identified several genes encoding ribosomal proteins and ribosome assembly factors as mild high-copy suppressors of the toxic Ppz1 effect. Ppz1 binds to ribosomes engaged in translation and copurifies with diverse ribosomal proteins and translation factors. Ppz1 overexpression results in Gcn2-dependent increased phosphorylation of eIF2α at Ser-51. Consistently, deletion of *GCN2* partially suppresses the growth defect of a Ppz1 overexpressing strain. We propose that the deleterious effects of Ppz1 overexpression are in part due to alteration in normal protein synthesis.

Highlights

* High catalytic activity of Ppz1 is detrimental for cell growth.

* Overexpression of Ppz1 leads to Gcn2-dependent phosphorylation of eIF2α.

* Ppz1 interacts with ribosomal components.

* Excess of Ppz1 activity negatively affect the translation initiation process.

Abreviations

CoA, Coenzyme A; GFP, Green Fluorescent Protein; LB, Lysogeny Broth; MALDI-TOF, Matrix-Assisted Laser Desorption/Ionization-Time-Of-Flight; OD, Optical Density; PBS, Phosphate-Buffered Saline; PCR, Polymerase Chain Reaction; PPC, Phosphopantothenoylcysteine; PPCDC, Phosphopantothenoylcysteine decarboxylase; PVDF, Polyvinylidene Difluoride; RFP, Red Fluorescent Protein; SC, Synthetic medium; SDS-PAGE, Sodium Dodecyl Sulfate–Polyacrylamide Gel Electrophoresis; TCA, Trichloroacetic Acid; YP, Yeast extract Peptone; YPD, Yeast extract Peptone Dextrose.

1. INTRODUCTION

Ppz1 is a type 1-related Ser/Thr protein phosphatase only found in fungi [1,2]. In *Saccharomyces cerevisiae* the enzyme is a 692-residue protein composed of a C-terminal catalytic domain, about 60% identical to Glc7, the catalytic subunit of *bona fide* yeast PP1, and a long N-terminal segment (~350 residues) unrelated to other proteins [3,4]. The genome of *S. cerevisiae* contains a paralog, Ppz2, whose function is far less relevant [4,5]. Ppz1 plays a fundamental role in the maintenance of monovalent cation homeostasis; this occurs by two complementary mechanisms: the regulation of the influx of potassium through the high-affinity Trk transporters and the expression of the Na^+/K^+-ATPase encoded by the *ENA1* gene [6–9]. As a result, cells lacking Ppz1 are hypertolerant to Na^+ and Li^+ cations, and sensitive to conditions or drugs affecting cell wall integrity [4,6,10,11]. More recently, Ppz1 has been involved in the regulation of endocytic trafficking and ubiquitin turnover through dephosphorylation of ubiquitin Ser-57 [12].

The activity of Ppz1 is regulated by its inhibitory subunits Hal3 and Vhs3 (being the action of Hal3 more relevant *in vivo*), which bind to the catalytic domain of the phosphatase [10,13–16]. In *S. cerevisiae* and other related fungi, Hal3 and Vhs3 are moonlighting proteins that play a key role in the formation of an atypical heterotrimeric phosphopantothenoylcysteine decarboxylase (PPCDC) enzyme [17] and, hence, in the biosynthesis of coenzyme A (CoA). Such heterotrimeric enzyme is made up of an essential Cab3 subunit plus Hal3 or/and Vhs3 subunits. This CoA-related function explains why *hal3*Δ *vhs3*Δ double mutant cells are not viable [13].

The activity of Ppz1 must be finely regulated in the cell since an abnormal increase in the level of the protein impairs cell growth. This was observed long ago when Ppz1 was expressed from an episomal plasmid driven either by the strong inducible *GAL1-10* or by its cognate promoter [10,18]. Further research indicated that high levels of Ppz1 cause a delay in the G_1/S transition of the cell cycle and in the expression of G_1 phase cyclins Cln2 and Clb5. Furthermore, the Ppz1-induced growth defect was completely rescued by the concomitant high dosage of the *HAL3* gene [19]. A shift toward the G_1 phase of the cell cycle has

been subsequently confirmed by a high throughput flow cytometry screen in a W303-derivative strain using *GAL1-10*-driven overexpression of Ppz1 [20].

However, beside this evidence, the actual reasons for Ppz1 toxicity have not been precisely clarified and the authentic cellular targets of this phosphatase are largely unknown. Remarkably, a recent genome-wide study using the genetic tug-of-war (gTOW) approach to identify dosage-sensitive genes revealed that *PPZ1* is the gene for which the cell has the lowest tolerance limit [21], thus suggesting that Ppz1 is likely the most toxic protein when overexpressed in budding yeast. Given the importance of *S. cerevisiae* both as biological research model and as organism of biotechnological relevance, and the relatively scarce knowledge about the cellular targets of the Ppz1 phosphatase, we considered relevant to investigate the molecular grounds for its extraordinary cellular toxicity. In this work, we have generated several tools that allow regulated expression of Ppz1 and we have demonstrated that the toxic effect of the overexpression of Ppz1 is due to an increase in its catalytic activity and not to down-titration of its regulatory subunits Hal3 and Vhs3, resulting in impaired CoA biosynthesis. Furthermore, we show that Ppz1 interacts with diverse ribosomal components and that an excess of Ppz1 activity results in polysome depletion and phosphorylation of the translation initiation factor eIF2α at its serine 51. All these results point to an impact of Ppz1 overexpression on translation initiation that partially explains the observed cell growth blockage. Therefore, the use of genetic tools that allow overexpression of Ppz1 (somehow equivalent to a gain of function mutation) could help to understand the physiological functions of this specific phosphatase.

2. MATERIAL AND METHODS

2.1. Growth of yeast strains

Yeast cells were incubated at 28°C in YP medium (1% yeast extract, 2% peptone) or in synthetic medium (SC) lacking the appropriate selection requirements [22], supplemented with a carbon source such as glucose (Glu, as in YPD), raffinose (Raff) or galactose (Gal), as indicated, at 2% unless otherwise stated. Plates contained 2% agar. Yeast strains used in the present study are

defined in Table 1. Transformed yeast cells containing *PPZ1* under the control of any doxycycline-repressible promoter were always plated in medium containing doxycycline (100 µg/ml).

Growth assays in liquid medium were performed in 96-well plates. Wild-type BY4741, *ppz1* and ZCZ01 strains were grown in YPD medium overnight, and then transferred to YP Raffinose containing diverse amounts of galactose at initial OD_{600} of 0.004. After 24 hours of growth at 28°C, the OD_{600} of the plates was measured by a Multiskan Ascent plate reader (Thermo Electron Corporation).

Flow cytometry measurements were performed in asynchronous cultures of cells growing on YP-Raffinose at different times after the addition of 2% galactose, using propidium iodide (0.5 mg/ml) to stain DNA, essentially as previously described [23].

2.2. DNA techniques and plasmid constructions

E. coli DH5α cells were used as plasmid DNA host and were grown at 37°C in LB medium supplemented with 50 µg/ml ampicillin, when required. Transformations of *S. cerevisiae* and *E. coli* and standard recombinant DNA techniques were performed as described [24].

The strain ZCZ01 was made by transforming BY4741 cells with a *kanMX6-GAL1-10* cassette amplified from plasmid pFA6a-kanMX6-pGAL1 [25] using oligonucleotides PPZ1_F4 and PPZ1_R2 (Table S1). Recombinants carrying the marker module were selected by resistance to 200 µg/ml G418, and correct insertion at positions -50 to -5 relative to the ATG initiating codon was subsequently confirmed by PCR using oligonucleotides E1_kpnI and K3. To prepare the MLM03 and MLM04 strains, the *kanMX4-Tta-TetO$_2$* and *kanMX4-Tta-TetO$_7$* cassettes were PCR-amplified from plasmids pCM224 and pCM225 [26], respectively, using the pair of oligonucleotides OMLM1 and OMLM2. BY4741 yeast cells were transformed with the 3.8 kb *kanMX4-Tta-tetO$_2$* or 4.0 kb *kanMX4-Tta-tetO$_7$* PCR products and cells containing the corresponding cassette inserted between nucleotides -51 and -5 relative to the initial *PPZ1* ATG initiating codon were selected in the presence of G418 to give rise to strains MLM03 (*tetO$_2$*) and MLM04 (*tetO$_7$*). The presence of the inserted cassette and the absence of the deleted promoter region were verified by PCR using primers OMLM5, OMLM6

and K2 (Table S1). Strains CCP05, CCP06, CCP08, CCP09 were constructed by transformation of wild-type strain BY4741 with a disruption cassette amplified from the *gal4*::*kanMX4* (2.7-kb), *gal11*::*kanMX4* (2.7-kb), *pgd1*::*kanMX4* (2.9-kb) and *med2*::*kanMX4* (3.2-kb) mutants from the systematic disruption collection in the BY4741 background [27]. The *gcn2*::*kanMX4* strain is a meiotic null segregant of the diploid strain Y23642 (Euroscarf).

Plasmids pCM188-PPZ1, pCM189-PPZ1 and pCM190-PPZ1 used to overexpress Ppz1 were obtained by cloning the 2.1 kb PCR-amplified fragment of the *PPZ1* ORF, using oligonucleotides OMLM3 and OMLM4, into the BamHI/PstI sites of pCM188, pCM189 and pCM190 vectors [28], respectively. Plasmids pEGH-Ppz1^{R451L} and pYES2-Ppz1^{R451L} were obtained replacing the 625-bp *Kpn*2I/*PacI* fragment in pEGH-PPZ1 or pYES2-PPZ1 (Table S2), respectively, with the same restriction fragment from previously described YCp111-Ppz1^{R451L} [18]. Other plasmids made in this study previously reported are described in Table S2.

2.3. Screening for multicopy suppressors of the lack of growth of the MLM04 strain

MLM04 cells were transformed with either YEp13- or YEp24-based yeast genomic DNA libraries and plated in the appropriate synthetic medium lacking uracil or leucine, as needed. Transformed cells were split in two identical aliquots to be plated onto plates containing 0.5% or 0.25% glucose. We analyzed a total number of 101,600 transformants with the YEp13 and 314,500 transformants with the YEp24-based library. Plasmids from positive clones were isolated, digested to identify empty and *HAL3*-containing vectors (that were discarded) and used to re-transform MLM04 cells. The specific ORFs present in each positive clone in this second round were deduced by DNA sequencing of both ends of the insert. Every single ORF was cloned, with its own promoter, into the YEp195 plasmid, either by restriction with the appropriate enzymes or by PCR amplification and re-tested in a newly transformed MLM04 strain. Details of the cloning into YEp195 are given in the Supplemental Information.

2.4. GST-Ppz1 pull down

With the objective to identify proteins interacting with Ppz1 *in vivo*, we overexpressed a GST-Ppz1^{R451L} version (lacking phosphatase activity) and GST, as control, from the galactose-inducible pEGH plasmid in the BY4741 strain. Transformants were grown in 150 ml of synthetic medium lacking uracil and with raffinose as carbon source to an OD_{600} of 0.6-0.8. Then, galactose was added to a final concentration of 2%. After 60 minutes, cells were recovered by filtration on 25 µm membranes (GN-6. Pall Corporation) and frozen. We used glutathione-affinity purification, as indicated in the Supplemental Information, to pull-down proteins associated with GST and with GST-Ppz1^{R451L}. Purified GST, GST-Ppz1^{R451L} and their bound proteins were subjected to SDS-PAGE [29]. Slices of the gel containing visible Coomassie blue-stained protein bands corresponding to GST-Ppz1^{R451L}-bound proteins were excised from the gel. The equivalent regions were also excised from the GST pull-down sample as a negative control. Tryptic peptides were identified by MALDI-TOF mass spectrometry at UAB facilities. Fragments cut from the same polyacrylamide gel, in a lane where no sample was loaded, were used as blank. Details for trypsin digestion and mass spectrometry analysis are given in Supplementary Materials.

2.5. Polysome preparations

Overnight culture of wild-type and MLM04 cells (5 ml) in SC medium lacking uracil with 100 µg/ml of doxycycline were washed twice with the same medium lacking doxycycline, resuspended in 10 ml of this medium and grown for 24 h. Cells were then brought to an OD_{600} of 0.2 in 200 ml of the medium and further incubated until the cultures reached OD_{600} of 0.8. Immediately before harvesting cycloheximide was added to a final concentration of 0.1 mg/ml. Polysome preparations were done essentially as in [30] except that 10 A_{260} units were used for sucrose gradient centrifugation. An Isco UV-6 gradient collector (Teledyne Isco, Lincoln, NE) with continuous monitoring at A_{254} was used to record the data. When needed, fractions of 0.5 ml were collected from the gradients and proteins extracted (see below).

2.6. Sample collection and preparation of protein extracts for immunoblot

Yeast crude extracts for immunodetection were prepared as follows. For monitoring Ppz1 levels in the ZCZ01 strain or in BY4741 cells carrying the pYES2-PPZ1 or GST-PPZ1^{R451L} plasmids, cells were incubated at 28°C in YP or in synthetic medium lacking uracil plus raffinose (2%), respectively, until OD_{600} 0.6-0.8. Samples of 10 ml were collected before and at specified time-points after addition of galactose (2% final concentration, unless otherwise stated). For detection of Ppz1 from pCM-based vectors and strain MLM04, cells were cultured as for polysome preparation, except that samples were taken after doxycycline removal as indicated. Protein extracts were prepared as described in [15]. Briefly, the cell pellets were resuspended in 125 µl of Lysis Buffer A supplemented with 0.1% Triton X-100, and 2 mM dithiothreitol (DTT), and 125 µl of Zirconia 0.5 mm beads were added. Cells were disrupted by vigorous shaking using a FastPrep cell breaker at setting 5.5 for 45 seconds (3 cycles). Samples were centrifuged at 500 x*g* for 10 min at 4°C and the total protein of the cleared supernatants quantified by the Bradford method (Sigma Chemical Co).

To analyze the phosphorylation state of eIF2α, BY4741 and ZCZ01 strains were grown, harvested and processed as described above, except that Lysis Buffer B (50 mM Tris-HCl, pH 7.5, 150 mM NaCl, 15% glycerol, 0.5% Tween-20, Phosphatase Inhibitor Cocktail Set V (Millipore) and EDTA-free Protease Inhibitor Cocktail (Roche)) was used.

Protein extracts from sucrose gradient fractions (0.5 ml) were obtained using the TCA/Acetone method. Briefly, 100 µL of trichloroacetic acid 100% was added to each sample, chilled on ice for 10 minutes and centrifuged at 13,000 x*g* for 10 min at 4°C. The supernatant was discarded, and pellets were washed twice with 1 ml of pre-chilled acetone, dried and resuspended in 25 µl of SDS-PAGE loading buffer.

2.7. SDS-PAGE and immunodetection

Unless otherwise stated, protein extracts were mixed with 4x SDS-PAGE loading buffer to yield a final concentration of 1x, heated for 5 minutes at 95°C, and resolved by SDS-PAGE at a concentration of 10% of polyacrylamide. Proteins were transferred onto polyvinylidene difluoride (PVDF) membranes (Immobilon-P, Millipore).

Ppz1 and Hal3 proteins were detected using polyclonal anti GST-Ppz1 [3], or anti Hal3 [10,31] antibodies at a 1:250 dilution and 1:500 dilution, respectively. The ribosomal proteins Rps8 and Rpl14 were detected using specific antibodies [32] at a 1:5000 dilution. The phosphorylated form of eIF2α was monitored with anti phospho-eIF2α (Ser-51) antibodies (Cell Signaling Technologies) at a 1:1000 dilution. A 1:20,000 dilution of secondary anti-rabbit IgG-horseradish peroxidase antibodies (GE Healthcare) was used in all cases. Immunoreactive proteins were visualized using the ECL Prime Western blotting detection kit (GE Healthcare) and chemiluminescence was detected in a Versadoc 4000 MP imaging system (BioRad). Membranes were stained with Ponceau Red to monitor proper loading and transfer.

2.8. Microscopy techniques

To monitor localization of Rps3-GFP, Rpl25-GFP and RFP-Nop1, strains BY4741, MLM04 and *ppz1* were grown until OD_{600} of 0.6-0.8 in the absence of doxycycline as described for polysome preparation. Yeast cells were fixed with a 2% formaldehyde solution at room temperature for 5 minutes, then centrifuged at 1,000 x*g* for 2 minutes, washed twice with PBS, and finally resuspended in PBS. Four µl of cells were deposited on a glass slide, covered with the coverslip and sealed with nail polish. The visualization of samples was done with the 100x objective using a Nikon Eclipse E-800 microscope. The FITC (ex: 480/30 nm, em: 535/45 nm) and the G-2A (ex: 435/50 nm, em: 580 nm) filters were used to visualize GFP and RFP, respectively.

2.9. RNA extractions and northern hybridization analyses

Saturated cultures of BY4741 cells containing the empty pCM190 vector (as a control) or pCM190-PPZ1 were prepared in SC lacking uracil in the presence of doxycycline, diluted to OD_{600} 0.2 in the same medium in the absence of doxycycline and growth continued for 8.5 h. Samples (10 OD_{600} units) were then taken at different times and total RNA was purified by the hot acid-phenol method [33]. Northern hybridization analysis was carried out as previously described [34,35]. Equal amounts of total RNA were loaded on 7% polyacrylamide-8 M urea gels (for the 5.8 and 5S probes) or 1.2% agarose-6%

formaldehyde gels (for the rest of probes) as previously described [35]. Specific [γ-^{32}P] ATP 5'-end labelled oligonucleotides (Table S3) were used as probes. Hybridization signals were detected using a TyphoonTM FLA9400 imaging system (GE Healthcare).

3. RESULTS

3.1. Construction and characterization of a galactose induced Ppz1 strain

To study the effects of increased dosage of *PPZ1,* we generated a yeast strain (ZCZ01) in which the proximal region of the *PPZ1* native 5'-untranslated region (from nt -5 to -50) was replaced by a cassette containing the *kanMX6* marker and the strong galactose-inducible *GAL1-10* promoter (see Table 1). Correct insertion of the cassette was PCR-verified and induction of *PPZ1* expression by 2% galactose was assessed by immunodetection of Ppz1 in whole cell extracts of ZCZ01 cells. As observed in Fig. 1A, Ppz1 is undetectable when ZCZ01 cells were grown on media containing raffinose as a carbon source (that is, its levels are lower than that in wild-type cells, compare time points at 0 h). Upon addition of 2% galactose to the medium, Ppz1 was immunodetected already 30 min after induction, and the levels of the phosphatase reached a plateau after 1-2 h. Fine tuning of Ppz1 expression could be achieved by using different amounts of the inductor, and high Ppz1 levels lasted for at least 20 h upon induction (Fig. 1B, upper panel). Growth of the ZCZ01 strain was inversely related to the expression level of Ppz1 and under strong overexpression conditions (> 0.05% galactose) it was drastically arrested, as observed in both liquid (Fig. 1B, bottom panel) and semi-solid cultures (Fig. 2A, B). Flow cytometry analysis of propidium iodide stained cells was used to quantitate the number of cells with one or two contents of DNA. The results clearly indicate that, after 4 h of Ppz1 overexpression, cells became arrested in G_1 phase, failing to duplicate their genome (Fig. 1C), in agreement with the delayed G_1/S transition described in cells overexpressing Ppz1 from its own promoter in multicopy plasmids [19]. This feature was accompanied by a marked increase in the percentage of unbudded cells, from 50.9 ± 3.0 to 88.4 ± 2.0 (mean ± SEM, n=3). It should be

noted that while overexpression of Ppz1 causes a severe block in growth, it does not result in cell death. As shown in Fig. 1D, ZCZ01 cells exposed for 20 h to galactose were able to resume growth when transferred to glucose or raffinose. Altogether, these results confirm that the overexpression of Ppz1 in the ZCZ01 strain perfectly reproduces the previously characterized growth defects identified upon overexpression driven from a *GAL1-10* promoter multicopy plasmid [18].

3.2. The deleterious effect of high levels of Ppz1 is due to increased phosphatase activity

Cellular toxicity as a result of overexpression of an enzymatic protein would be considered, in most circumstances, indissolubly associated to an undesirable increase in its enzymatic activity (protein phosphatase, in our case). However, the moonlighting nature of the Ppz1 regulatory subunits, Hal3 and Vhs3, introduced an additional factor. Indeed, it had to be considered the possibility that the excess of Ppz1 protein might sequester available Hal3 and Vhs3, thus interfering with proper PPCDC formation and subsequent CoA biosynthesis. To confirm or discard this latter possibility, we carried out different experiments. Firstly, we overexpressed in wild-type cells a version of Ppz1 that carries the R451L mutation, which strongly impairs its catalytic activity [18]. As shown in Fig. 2A (upper panel), expression of this version results far less toxic to the cell than expression of the native enzyme from the same vector, even when the phosphatase variant is expressed at much higher levels than the native protein (Fig. 2A, lower panel). Second, we transformed strain ZCZ01 with high copy-number plasmids harboring the *HAL3* and *VHS3* genes. As previously observed for the expression of *PPZ1* driven from its own promoter in an episomal plasmid [10], overexpression of Hal3 fully counteracted that of Ppz1. Overexpression of Vhs3 was also beneficial, although the effect was less patent than in the case of Hal3 (Fig. 2B). As overexpression of Hal3 or Vhs3 would also provide effective PPCDC components, thus leaving open the possibility that excessive Ppz1 could interfere with CoA biosynthesis, we also transformed strain ZCZ01 with different mutated versions of Hal3. Our results showed that the versions with strongly impaired capacity to bind to and/or to inhibit Ppz1, such as $Hal3^{W452G}$ or $Hal3^{E460G}$, were unable to rescue the growth defect of Ppz1

overexpressing cells or did it very poorly (Fig. S1), pointing again to the relevance of Ppz1 activity. Finally, we transformed strain ZCZ01 with plasmid pRS699-HsHal3. This vector allows potent expression of human PPCDC (HsCoaC), which provides full decarboxylase function in yeast. This protein is able to rescue the lethality of a triple *hal3 vhs3 cab3* mutation, while it is totally ineffective as inhibitor of Ppz1 [17]. As observed in Fig. 2B, overexpression of the human PPCDC enzyme was completely ineffective in rescuing Ppz1 toxicity. Taken together, all these results indicate that the negative effect of Ppz1 overexpression derives from an undesirable increase in its protein phosphatase activity.

3.3. Generation and characterization of new yeast strains containing *tetO*-regulatable *PPZ1.*

We first transformed the EUROFAN knockout collection with the pYES2-PPZ1 plasmid, in which *PPZ1* expression is controlled by the *GAL1-10* inducible promoter. We expected to recover mutations involved in the direct suppression of toxicity when Ppz1 is overexpressed. Five positive mutant strains able to grow upon transformation with the pYES2-PPZ1 plasmid were found: two of them carried null alleles of the *GAL3* and *GAL4* genes, which are direct transcriptional activators of the *GAL1-10* promoter. The other suppressor mutants were *gal11*Δ, *pgd1*Δ and *med2*Δ*,* all of them involved in the Mediator complex functions. These three mutants have been also reported as deficient in galactose-driven induction [36–38]. Consequently, all five mutations affected the ability to overexpress Ppz1 from the *GAL1-10* promoter, as verified by immunoblot analysis (Fig. S2).

Due to the inability to identify actual suppressor mutations for Ppz1 toxicity, we undertook a second genome-wide approach based in a screen for high-copy number suppressors of the Ppz1-induced growth defect. We reasoned that, due to the high toxicity of the phosphatase, the strong Ppz1 expression achieved in the ZCZ01 strain could make difficult the identification of high-copy suppressors. Therefore, we decided to use a system yielding lower levels of the phosphatase. To this end, we constructed two yeast strains, MLM03 and MLM04 (Table 1), in which the *PPZ1* coding region was placed under the control of the doxycycline-repressive *tetO* promoter, harboring two or seven *tetO* boxes, respectively.

Growth of strains MLM03 and MLM04 in synthetic solid medium was not affected by the presence of doxycycline (Fig. 3A). As shown in Fig. 3B, removal of doxycycline led to overexpression of *PPZ1*. It must be noted that, in this cell model, expression of Ppz1 takes longer and the levels reached are lower (compare with non-induced cells) than in ZCZ01 cells. Interestingly, the slow growth phenotype of MLM03 and MLM04 cells was glucose-dependent. Virtually, no effect on cell growth was detected in plates containing 2% glucose in the absence of doxycycline, but growth was drastically affected when glucose was lowered to 0.25% (Fig. 3A). In fact, these strains did not grow in alternative non-fermentable carbon sources (Fig. S3). This effect was more evident in MLM04 than in MLM03 cells, consistent with the higher potency of the promoter in the former strain. Lack of growth of MLM03 and MLM04 cells was even more evident when the medium contained 2% of galactose as the only carbon source (Fig. 3A). As observed previously in ZCZ01 cells, overexpression of *HAL3* also counteracted the toxicity of Ppz1 in both MLM03 and MLM04 cells even when galactose was used as carbon source. In fact, the presence of high levels of Hal3 allowed cells to increase the amount of expressed Ppz1 (Fig. 3B), suggesting that the increase in phosphatase activity was effectively counteracted.

3.4. A screen for high-copy number suppressors of Ppz1 toxicity uncovers genes involved in protein translation.

Based on the results shown in section 3.3, we considered that the newly generated strains would be more appropriate for the search of high-copy number suppressors of Ppz1 toxicity since they would not only provide lower Ppz1 levels, but also allow to avoid the use of galactose as inductor, which might not have a neutral effect on cell growth. Therefore, the screen was carried out using medium containing 0.5 or 0.25% glucose, which are conditions that substantially affect growth of the MLM04 strain in the absence of doxycycline (Fig. 3A). Nine suppressor genes able to improve, at some degree, the growth of cells overexpressing *PPZ1* in medium containing 0.25% glucose were obtained (Fig. 4A and Table 2). Expression of the selected suppressors did not decrease the expression levels of the *tetO*$_7$-driven *PPZ1*, even when expression was carried out from the pCM190-PPZ1 plasmid, an episomal vector expressing *PPZ1* from

the *tetO*$_7$-regulated promoter in the absence of doxycycline (Fig. S4). Two of the found suppressors were related to the sporulation process (*SPO20* and *SWM1*), two others were related to the biogenesis of ribosomes (*NOC2* and *DOT6*) and the remaining five encoded ribosomal proteins from both ribosomal subunits (*RPS6A*, *RPS15*, *RPP2A*, *RPL37A* and *RPL37B*). None of the suppressors was able to allow growth of the MLM04 strain in the presence of galactose, except for *NOC2*, which allowed slight growth only discernable after five or more days of incubation (Figure 4B). These results suggest that overexpression of Ppz1 could alter normal ribosomal synthesis or function and that this anomaly is partially alleviated by the overexpression of some proteins constituents of the ribosome or involved in its biogenesis.

To identify a possible additive suppressor effect when two suppressor genes were simultaneously overexpressed we transformed MLM04 cells with each combination of suppressors (including Hal3 as positive reference), one cloned into the high-copy plasmid YEp181 and the second into the high-copy plasmid YEp195. In the presence of 0.25% glucose, the strongest effect was observed when *SWM1* was co-expressed with *DOT6*, *RPL37A* or *RPS6A*. A slighter interaction was detected between *RPS15* and the other genes encoding ribosomal subunits. Interestingly, no additivity was found between *SWM1* and *SPO20* (Fig. 4C and Table S4). None of the suppressors was able to enhance the effect of *NOC2*. The interaction landscape showed some distinctive traits when cells were grown in the presence of galactose. In this case, no interaction between genes encoding ribosomal proteins was observed. Co-expression of *NOC2* with *RPS6A*, *RPL37A* and *RPP2A*, as well as with *SWM1* and *SPO20*, was additive. As observed in 0.25% glucose, no additivity was detected between *NOC2* and *DOT6,* nor between *SWM1* and *SPO20* (Fig. 4C and Table S5). It is worth noting that most interactions take place between genes encoding proteins involved in different functional categories.

3.5. GST-Ppz1 copurifies with diverse proteins involved in translation

As a parallel approach to identify new possible functions of Ppz1, we determined the set of proteins specifically co-purifying with this phosphatase. For this purpose, GST and the catalytically inactive version GST-Ppz1^{R451L} (this

variant was used to allow sufficient level of Ppz1 expression) were purified from yeast cells and subjected to SDS-PAGE. Slices of the gel containing visible Coomassie-stained bands (see Fig. 5A) were subjected to tryptic digestion and the sequence of the peptides determined by mass spectrometry. The equivalent gels section from GST pull-downs purified in identical manner were also sliced and analyzed as controls. As detailed in Table S6, we have identified several specific GST-Ppz1-bound proteins involved in the translation process that are not found in the control samples. These are the translation elongation factor EF-1α (Tef1/Tef2), and up to five proteins from the large ribosomal subunit: Rpl3, Rpl4A (most peptides also correspond to Rpl4B), Rpl13B (most peptides were identical to Rpl13A), Rpl10 and Rpl2A/Rpl2B. The detected interactions of Ppz1 with a translation elongation factor and several ribosomal proteins further support the notion that this phosphatase might have a relevant impact in the translation process.

3.6. Excess of Ppz1 alters normal polysome profile

Because of the known role of Noc2 and Dot6 in ribosome biogenesis, we analyzed by northern blot, using probes described in Table S3, the processing of the rRNAs in cells expressing *PPZ1* from the pCM190 plasmid after removal of doxycycline. However, we did not observe drastic alterations in the pre-rRNA maturation process affecting neither the 40S nor the 60S subunit synthesis pathways during the induction of Ppz1 (Fig. S5; compare times 0 and 6h). Thus, the excess of Ppz1 does not seems to impair significantly pre-rRNA processing. Next, we investigated the ribonucleoprotein maturation/transport process. This was done by monitoring by fluorescence microscopy the transport from the nucleus to the cytoplasm of pre-ribosomal particles containing tagged small (Rps3-GFP) and large (Rpl25-GFP) ribosomal subunits. mRFP-Nop1 was employed as a marker for nucleolar localization. Comparison of the localization of these proteins in a wild-type strain with that of MLM04 cells after long-term incubation without doxycycline (28 h) showed no differences in the localization of these proteins, which were cytosolic in both cases (Fig. S6). Localization of the ribosomal proteins was also unaffected in a *ppz1*Δ mutant strain. Thus, over-

expression of *PPZ1* does not affect neither the rRNA maturation process nor the export of ribosomal subunits from the nucleolus to the cytoplasm.

We next investigated whether over-expression of Ppz1 interferes with the translation process. To do so, we compared the polysome profiles of the MLM04 strain in the absence of doxycycline with those obtained from an isogenic wild-type counterpart grown in the same conditions. As shown in Fig. 5B, MLM04 cells showed a clear reduction in the polysome content when compared to the wild-type strain; thus, the polysome-to-monosome ratio decreased from ca. 1.5 in wild-type to 1.1 in MLM04 cells. This result is compatible with a mild impairment of the translation initiation process upon overexpression of Ppz1. Reduced polysomal content was also observed when *PPZ1* was overexpressed from a high copy number pCM190 plasmid (not shown), confirming that the excess of Ppz1 activity somehow impairs the translation process. Consistently with a direct interference of increased Ppz1 phosphatase activity on translation, overexpression of the Ppz1 inhibitor Hal3 from the episomal YEp195 plasmid normalized the altered pattern observed in MLM04 cells (Fig. 5B).

Remarkably, endogenous Ppz1 was found in numerous polysomal fractions, as deduced from immunoblot of samples from BY4741 cells transformed with the empty pCM190 plasmid (Fig. 5C). Similarly, Ppz1 was also immunodetected in all polysomal fractions, as well as in other fractions containing ribosomal particles in BY4741 cells transformed with pCM190-PPZ1 (not shown). Fig. 5D shows the distribution of Ppz1 in fractions of polysome preparations obtained from MLM04 cells overexpressing Hal3. Interestingly, Ppz1 and Hal3 distribution is not the same, since Hal3 is largely concentrated in fractions 1 to 3, corresponding to free (soluble) material. The different polysomic distribution of Ppz1 and Hal3 suggests that the polysome-associated Ppz1 would not be inhibited by Hal3 and, therefore, be active as phosphatase. As it can be seen, overexpression of Hal3 does not lead to the eviction of Ppz1 from translating ribosomes. However, Ppz1 seems to accumulate somewhat in non-polysomal fractions when Hal3 is overexpressed.

3.7. eIF2α is hyper-phosphorylated in cells overexpressing Ppz1

Global regulation of translation involves two major inhibitory mechanisms, the phosphorylation of eIF2α at its conserved Ser-51, which impairs the regeneration of GTP-bound eIF2 and the sequestering of eIF4E as a translation-unproductive complex by the eIF4E-binding proteins (4E-BPs). In yeast, the non-essential Gcn2 is the sole kinase described to phosphorylate eIF2α (Sui2) [39], while two non-essential 4E-BPs, Eap1 and Caf20, have been described [40–42]. We then monitored the phosphorylation state of eIF2α when *PPZ1* was overexpressed by using a phospho-specific antibody against the phosphorylated Ser-51. As shown in Fig. 6A, overexpression of Ppz1 in strain ZCZ01 led to a long-term (4h) phosphorylation of eIF2α. Consistent with the major role of Gcn2 on phosphorylation of eIF2α, deletion of *GCN2* fully abolished phosphorylation of eIF2α in Ppz1-overexpressing cells (Fig. 6B). Thus, we can conclude that hyperphosphorylation of eIF2α at Ser-51 triggered by overexpression of *PPZ1* is dependent on Gcn2. We wondered up to what extent phoshorylation of eIF2α could be responsible for the dramatic growth defect due to strong Ppz1 overexpression. Cells overexpressing Ppz1 from pYES2-PPZ1 and deleted for *GCN2* were still unable to grow (not shown). We then investigated the effect of lack of Gcn2 resorting to a set of *tetO*-based plasmid expression vectors to allow fine-tuning the expression level of Ppz1. The weakest was pCM188 (*tetO*$_2$, centromeric); pCM189 (*tetO*$_7$, centromeric) allowed intermediary expression levels, and pCM190, already described above, led to the strongest expression. As observed in Fig. 6C, expression of Ppz1 from these vectors results in a glucose-dependent growth defect, as previously observed for strain MLM03 and MLM04 (see Fig. 3A). As it can be seen, the intensity of the phenotype correlates with the expected expression level. In all three conditions, deletion of *GCN2* resulted in noticeable improvement in growth (Fig. 6C), indicating that at these levels of expression, phosphorylation of eIF2α partially contributes to the observed growth defect.

We also tested whether deletion of *EAP1* and *CAF20* might improve growth in Ppz1-overexpressing cells. However, deletion of none of these genes or even the double mutation did not improve growth at all when Ppz1 was expressed from any of the pCM-derived vectors (Fig. S7). These results suggest that the excess of Ppz1 does affect phosphorylation of eIF2α but does not seem to induce a

translation initiation defect by increasing the sequestering of eIF4E by either Caf20 or Eap1.

4. DISCUSSION

Ppz1 is a fungus-specific protein phosphatase that was identified, when overexpressed, as the most toxic yeast protein [21]. Since Ppz1 was suggested as potential target for antifungal therapy [43–45], we decided to shed light on the causes of this toxicity. We have previously demonstrated that the inhibitory subunits of Ppz1 also contribute to the PPCDC activity [17], required for the synthesis of CoA, an essential cellular function. We used the ZCZ01 strain to test whether toxicity was due to an excess of Ppz1 catalytic activity or because the overexpressed Ppz1 titrated down its negative regulators, compromising thus the synthesis of CoA. Our results demonstrate that the excess of catalytic activity is at the basis of Ppz1 overexpression toxicity. This assertion is based in that: i) growth is restored when the overexpressed Ppz1 is a catalytically inactive version (Fig. 2A); ii) overexpression of Vhs3, which has a lesser capacity than Hal3 to inhibit Ppz1 [13], was less effective to overcome the growth arrest due to Ppz1 overexpression (Fig. 2B); iii) overexpression of Hal3 versions defective in their ability to inhibit Ppz1 [46] were ineffective as suppressors of the cell growth blockage caused by excess of Ppz1 (Fig. S1); iv) Human HsCoaC, reported as a functional PPCDC in *S. cerevisiae* [17], was totally ineffective in rescuing the deleterious phenotype caused by excess of Ppz1 (Fig. 2B). It must be noted that the earlier observation that overexpression of the phosphatase domain of Ppz1 also blocks growth [18] could not be taken as evidence to support the role of the catalytic activity in toxicity, since the catalytic domain binds Hal3 even stronger than the entire protein [10].

We have used a *GAL1-10* promoter-driven Ppz1 expression from a multicopy vector to transform and screen the knockout collection of mutants for non-essential genes whose deletion alleviated the lack of growth caused by overexpression of Ppz1. We reasoned that if hyper-dephosphorylation of a specific substrate by the overexpressed Ppz1 was deleterious for cell growth, it could be plausible that cells containing the deletion of this gene could grow better. This approach was not successful since all the mutants found in our screen

turned out to be required in the process of transcriptional activation by galactose, and therefore these mutants were unable to overexpress Ppz1 from the *GAL1-10* promoter (Fig. S2). We hypothesize that the failure to obtain hits using this strategy might be indicative of the existence of multiple relevant targets for the phosphatase, so loss of a single one would not be sufficient to allow rescue in the rather drastic conditions used in the screen. In fact, we show here that deletion of certain genes, such as *GCN2*, could only mildly alleviate the growth defect of cells overexpressing Ppz1.

The detrimental effect on cell growth upon *tetO*-driven Ppz1 overexpression from the episomal pCM190 vector was observed in six different wild-type strains, although the intensity of the effect was found to be strain-dependent, being more dramatic in YPH499, DBY746, JA100 and W303-1A than in BY4741 and KT112 strains (not shown). This could be caused by different levels of Ppz1 or by the differential sensitivity to Ppz1 overexpression in each strain. An unexpected finding using the *tetO* system is that the growth defect triggered by overexpression of Ppz1 depends on the availability of glucose, being maximized under glucose deprivation and particularly in the presence of galactose as sole carbon source (Fig. 3A, 6C and 7C). This result suggests that high levels of Ppz1 might affect the glucose sensing system or the proper cellular response to glucose starvation. This is a relevant finding that should be considered when interpreting other previous reports in which the *GAL1-10* promoter has been used to overexpress Ppz1. Multiple factors could negatively affect cell growth when Ppz1 is overexpressed in low-glucose medium. Excess of Ppz1 could, for example, take over the role of Glc7-Reg1, a phosphatase complex that dephosphorylates Snf1 kinase and its downstream transcriptional repressor Mig1, thus interfering with the mechanisms that allow adaptation to glucose scarcity [47]. This would explain the inability of MLM03 and MLM04 to grow on carbon sources other than glucose. Excess of Ppz1 activity could also interfere with the PKA or Sch9 pathways, which act in conjunction responding to glucose availability, having the latter a role as regulator of ribosome biogenesis [48–50]. Further investigations are required to explain these results.

We have found that Ppz1 co-purifies with several ribosomal proteins from the large subunit as well as with the translation elongation factor EF-1α. In addition, the translation elongation factor EF-3 (Yef3) was also identified by liquid

chromatography-MS/MS in an independent experiment that will be described elsewhere. So far, no physical interactions have been detected between Ppz1 and ribosomal proteins, according to the BioGrid database [51], although interactions with proteins directly or indirectly involved in several functions affecting the translation process, such as mRNA processing (Mud1, Pat1, Snp1, Snu66, Dhh1) and the export to cytosol of mRNAs and ribosomal subunits (Crm1, Nab2) have been described. Interestingly, EF-3 and EF-1α are involved in a common biological role, since EF-3 stimulates the function of EF-1α in the binding of the aa-tRNA to the ribosomal A-site. A recent proteomic-scale study showed that the deletion of the *C. albicans* ortholog of Ppz1 affected both, the cellular quantity and the phosphorylation levels of several ribosomal proteins as well as initiation and elongation factors [52]. All these pieces of information support a role of Ppz1 in regulating the translation process.

The notion that the translation process could be one of the targets responsible for the deleterious effect of Ppz1 overexpression was reinforced by: i) the results of our high copy number screen, in which overexpression of two proteins involved in ribosome biogenesis (Noc2 and Dot6) and of several ribosomal proteins improved growth to some extent (Table 2), and ii) the observation that overexpression of Ppz1 results in depletion of polysomes and hyperphoshorylation of eIF2α. In contrast, no changes were detected neither in pre-rRNA maturation nor in the nucleus to cytoplasm export of the small and large ribosomal subunits. Altered polysome profiles, similar to those observed in cells overexpressing Ppz1, have been previously shown upon partial loss-of-function and deletion of the genes *TIF1* and *TIF3*, encoding translation initiation factors eIF4A and eIF4B, respectively [30,53]. However, the growth defects of these mutants are not comparable to the drastic reduced growth observed upon overexpression of Ppz1. Since the altered polysome profile obtained for cells overexpressing Ppz1 is not sufficient to fully explain their observed growth defects, we conclude that the translation initiation process might not be the sole target responsible of Ppz1 toxicity. It is suggestive that overexpression of Hal3 displaces part of the Ppz1 population from polysomal to non-polysomal fractions (Fig. 5C & D). This might contribute to the beneficial effect caused by Hal3 overexpression.

Phosphorylation of eIF2α by the Gcn2 kinase is a key event in the downregulation of initiation of translation, related to the formation of the ternary complex. It is known that activation of Gcn2 occurs not only in response to uncharged tRNAs, but also takes place in cells subjected to different forms of stress [54,55]. In contrast, Caf20 and Eap1 are negative regulators of the formation of the closed loop complex [55,56]. Our observation that deletion of *GCN2* improves, up to some extent, growth of cells overexpressing Ppz1, but lack of Caf20 or/and Eap1 does not, suggests that the excess of Ppz1 affects the formation of the ternary complex rather than that of the closed-loop complex.

A relevant question is whether eIF2α is a *bona fide* Ppz1 substrate. It was reported long ago that Glc7 could act as eIF2α phosphatase [57] in a way that involves recruitment of the phosphatase by the N-terminus of eIF2γ [58]. It is evident that the effect of excess of Ppz1 activity on eIF2α must be indirect, since in this case the result is the hyperphosphorylation of the initiation factor. The notion that this phosphorylation could be a secondary effect is reinforced by the fact that it is observed well after expression of Ppz1 has been induced (4 h induction). In contrast, it is tempting to consider Gcn2 as a direct target of Ppz1. Although autophosphorylation of Gcn2 in its activation loop (Thr-882) is required for the activity, at least nine additional phospho-residues have been identified in this protein. It can be hypothesized that Ppz1 could be a direct Gcn2 phosphatase acting in any of these phosphorylation sites, and this dephosphorylation being required for Gcn2 activation. Since dephosphorylation of Ser-577 seems to be required to activate Gcn2 [59], this could be one of the potential targets of Ppz1. Alternatively, overexpression of Ppz1 could be affecting pathways upstream Gcn2, promoting any of the stress responses that leads to the activation of Gcn2. However, it should be noted that independent studies reported a strong negative genetic interaction between the *ppz1* and *gcn2* deletion mutant cells [60–62]. Such interaction cannot be explained within the context described above and is suggestive of Gcn2-independent effects of Ppz1 overexpression.

Preliminary experiments (not shown) suggest that the excess of Ppz1 does not cause translation misreading, so it seems evident that the impact of Ppz1 overexpression on translation is unrelated to the previously reported role of Ppz1 on translational fidelity through the regulation of Tef5, the GDP/GTP exchange subunit for the translation elongation factor EF-1A [63].

Early work suggested that episomal expression of the *PPZ1* gene resulted in delayed expression of the G_1 cyclins Cln2 and Clb5 and in arrest at the G_1 phase of the cell cycle [19]. Glc7 has also been involved in different steps of the cell cycle, including the dephosphorylation of targets of the Dbf4-dependent kinase (DDK) complex through the association with its Rif1 subunit, thus preventing entry into S phase [see [64] for a review]. It is worth noting that Ppz1 and Glc7 might not be fully insulated with respect to some specific functions and that Ppz1 could interact with certain Glc7 subunits, such as Glc8 and Ypi1 [65,66]. This might lead to the assumption that the harmful effect of Ppz1 overexpression mimics that of Glc7 and could be caused by dephosphorylation of Glc7 targets. However, a number of results do not support such assumption: i) overexpression of Glc7 from *GAL1-10* promoter has been reported to cause cell death [67,68]. In contrast, overexpression of Ppz1 does not result, at least at short-medium term, in reduced viability (Fig. 1D); ii) the delay in the G_1/S transition observed when Ppz1 is overexpressed differs from the mitotic exit defects observed under Glc7 overexpression [69,70]; iii) overexpression of Glc7 renders cells with abnormal morphology [70,71], not seen in Ppz1-overexpressing cells, and in chromosome instability [72,73], a phenotype that was not detected in the same studies when Ppz1 was overexpressed; iv) the profile of high-copy suppressors found in our study does not overlap with that identified by Ghosh and Cannon [68] and, in contrast to Glc7, we observed that the *glc8*Δ or *reg2*Δ mutations do not act as suppressors of *PPZ1*-induced lack of growth (not shown).

In summary, we show here that Ppz1 overexpression leads to a halt in translation initiation. However, although this effect could contribute to the growth defect in Ppz1 overexpressing cells, as deduced from the beneficial impact of the *GCN2* deletion, we do not believe it constitutes the primary reason. From one side, deletion of *GCN2* does not fully restore normal cell growth. On the other hand, the additive effect between suppressors with apparently unrelated functions (see Fig. 4B, C) suggest that the growth defect in Ppz1 overexpressing cells has not a single origin. Therefore, our results point to a scenario in which the excess of Ppz1 activity might affect numerous protein targets involved in different cellular functions, including protein translation. Ongoing work based on transcriptomic and phosphoproteomic studies may shed further light into these processes.

CONFLICT OF INTERESTS

The Authors declare no conflict of interests.

ACKNOWLEDGEMENTS

The technical assistance of Montserrat Robledo is acknowledged. We thank M. Albarcar for contribution to the characterization of the ZCZ01 strain, Dr. Megan Mayerle (C. Guthrie's laboratory, UCSF), J. Bassler and E. Hurt (Biochemistry Center, BZH, University of Heidelberg, Germany) for diverse plasmids, E. Matallana (IATA, Valencia, Spain) and G. Dieci (Università degli Studi di Parma, Italy) for the anti P-eIF2α antibody and anti Rps8 and anti Rpl14 antibodies, respectively, and G. Pavitt (The University of Manchester, UK) for the *caf20* and *eap1* mutant yeast strains. We thank SePBioEs and LP-CSIC/UAB facilities for mass spectrometry analyses. LP-CSIC/UAB is a member of Proteored.

This research was funded by grant BFU2017-82574-P to JA and AC, and BFU2016-75352-P to JdlC (AEI/FEDER, EU; Ministerio de Industria, Economía y Competitividad, Spain, and ERDF). CC and JF-F were recipient of a PhD fellowship from the Ministerio de Economía y Competitividad (Spain). CZ was recipient of a PhD fellowship from the China Scholarship Council. DV was recipient of a PhD fellowship from UAB.

TABLE 1. YEAST STRAINS

Name	Features	Reference or source
BY4741	MAT **a** *his3*Δ1 *leu2*Δ *met15*Δ *ura3*Δ	[74]
ZCZ01	BY4741 $_{p}$*GAL1-10:PPZ1*	This study
MLM03	BY4741 $_{prom}$*tetO$_2$:PPZ1*	This study
MLM04	BY4741 $_{prom}$*tetO$_7$:PPZ1*	This study
CCP05	BY4741 *gal4::kanMX4*	This study
CCP06	BY4741 *gal11::kanMX4*	This study
CCP08	BY4741 *pgd1::kanMX4*	This study
CCP09	BY4741 *med2::kanMX4*	This study
gcn2	BY4741 *gcn2::kanMX4*	This study
ppz1	BY4741 *ppz1::kanMX4*	EUROFAN
BY4742	MAT *α his3*Δ1 *leu2*Δ *lys2*Δ *ura3*Δ	[74]
Y17334	BY4742 *caf20*::*kanMX4*	[75]
Y17036	BY4742 *eap1*::*kanMX4*	[75]
GP6967	BY4742 *caf20*::*kanMX4 eap1*::*kanMX4*	G. D. Pavitt

TABLE 2. High-copy suppressor genes of Ppz1 toxicity. Genes identified from the YEp24-based library are denoted with an asterisk.

Gene	Protein description	Function
DOT6	rRNA and ribosome biogenesis.	Ribosome biogenesis
NOC2	Part of nucleolar complexes. Mediates intranuclear transport of ribosomal precursors. Associates with nascent pre-rRNA.	
RPS6A	Component of the small (40S) ribosomal subunit. Orthologous to mammalian ribosomal protein S6.	Ribosomal proteins
*RPS15**	Component of the small (40S) ribosomal subunit. Orthologous to mammalian ribosomal protein S15.	
RPL37A	Component of the large (60S) ribosomal subunit. Orthologous to mammalian ribosomal protein L37.	
RPL37B	Paralog of *RPL37A*.	
*RPP2A**	Ribosomal protein P2α involved in the interaction between translational elongation factors and the ribosome. Free P2 stimulates the phosphorylation of the eIF2α subunit by Gcn2.	
*SPO20**	Meiosis-specific subunit of the t-SNARE complex. Required for prospore membrane formation during sporulation.	Meiosis/ sporulation
SWM1	Subunit of the anaphase-promoting complex (APC). E3 ubiquitin ligase that regulates the metaphase-anaphase transition and exit from mitosis. Required for spore wall maturation.	Cell cycle/spore-wall formation

Protein descriptions and functions are extracted from the SGD Project webpage (http://www.yeastgenome.org) [76].

References

[1] J. Ariño, D. Velázquez, A. Casamayor, Ser/Thr protein phosphatases in fungi: structure, regulation and function, Microb. Cell. 6 (2019) 217–256. https://doi.org/10.15698/mic2019.05.677.

[2] J. Ariño, Novel protein phosphatases in yeast, Eur. J. Biochem. 269 (2002) 1072–1077.

[3] F. Posas, A. Casamayor, N. Morral, J. Ariño, Molecular cloning and analysis of a yeast protein phosphatase with an unusual amino-terminal region., J. Biol. Chem. 267 (1992) 11734–40. http://www.ncbi.nlm.nih.gov/pubmed/1318299.

[4] K.S. Lee, L.K. Hines, D.E. Levin, A pair of functionally redundant yeast genes (PPZ1 and PPZ2) encoding type 1-related protein phosphatases function within the PKC1-mediated pathway, Mol. Cell Biol. 13 (1993) 5843–5853. https://doi.org/10.1128/mcb.13.9.5843.

[5] F. Posas, A. Casamayor, J. Ariño, The PPZ protein phosphatases are involved in the maintenance of osmotic stability of yeast cells, FEBS Lett. 318 (1993) 282–286. https://doi.org/10.1016/0014-5793(93)80529-4.

[6] F. Posas, M. Camps, J. Ariño, The PPZ protein phosphatases are important determinants of salt tolerance in yeast cells., J. Biol. Chem. 270 (1995) 13036–13041. https://doi.org/10.1074/jbc.270.22.13036.

[7] A. Ruiz, L. Yenush, J. Arino, Regulation of ENA1 Na(+)-ATPase gene expression by the Ppz1 protein phosphatase is mediated by the calcineurin pathway, Eukaryot. Cell. 2 (2003) 937–948. https://doi.org/0.1128/ec.2.5.937-948.2003.

[8] L. Yenush, S. Merchan, J. Holmes, R. Serrano, pH-Responsive, Posttranslational Regulation of the Trk1 Potassium Transporter by the Type 1-Related Ppz1 Phosphatase, Mol Cell Biol. 25 (2005) 8683–8692. https://doi.org/10.1128/MCB.25.19.8683-8692.2005.

[9] L. Yenush, J.M. Mulet, J. Ariño, R. Serrano, The Ppz protein phosphatases are key regulators of K^+ and pH homeostasis: implications for salt tolerance, cell wall integrity and cell cycle progression., EMBO J. 21 (2002) 920–929. https://doi.org/10.1093/emboj/21.5.920.

[10] E. de Nadal, J. Clotet, F. Posas, R. Serrano, N. Gomez, J. Ariño, The yeast halotolerance determinant Hal3p is an inhibitory subunit of the Ppz1p Ser/Thr protein phosphatase., Proc. Natl. Acad. Sci. U. S. A. 95 (1998) 7357–62.

https://doi.org/0.1073/pnas.95.13.7357.

[11] S. Merchan, D. Bernal, R. Serrano, L. Yenush, Response of the Saccharomyces cerevisiae Mpk1 mitogen-activated protein kinase pathway to increases in internal turgor pressure caused by loss of Ppz protein phosphatases., Eukaryot Cell. 3 (2004) 100–107. https://doi.org/10.1128/ec.3.1.100-107.2004.

[12] S. Lee, J.M. Tumolo, A.C. Ehlinger, K.K. Jernigan, S.J. Qualls-Histed, P.-C. Hsu, W.H. McDonald, W.J. Chazin, J.A. MacGurn, Ubiquitin turnover and endocytic trafficking in yeast are regulated by Ser57 phosphorylation of ubiquitin, Elife. 6 (2017). https://doi.org/10.7554/eLife.29176.

[13] A. Ruiz, I. Muñoz, R. Serrano, A. Gonzalez, E. Simon, J. Arino, Functional characterization of the Saccharomyces cerevisiae VHS3 gene: a regulatory subunit of the Ppz1 protein phosphatase with novel, phosphatase-unrelated functions, J. Biol. Chem. 279 (2004) 34421–34430. https://doi.org/10.1074/jbc.M400572200.

[14] I. Muñoz, E. Simón, N. Casals, J. Clotet, J. Ariño, Identification of multicopy suppressors of cell cycle arrest at the G1 - S transition in Saccharomyces cerevisiae, Yeast. 20 (2003) 157–169. https://doi.org/10.1002/yea.938.

[15] J.A. Abrie, A. González, E. Strauss, J. Ariño, Functional mapping of the disparate activities of the yeast moonlighting protein Hal3., Biochem. J. 442 (2012) 357–68. https://doi.org/10.1042/BJ20111466.

[16] J.A. Abrie, C. Molero, J. Ariño, E. Strauss, Complex stability and dynamic subunit interchange modulates the disparate activities of the yeast moonlighting proteins Hal3 and Vhs3, Sci. Rep. 5 (2015). https://doi.org/10.1038/srep15774.

[17] A. Ruiz, A. Gonzalez, I. Munoz, R. Serrano, J.A. Abrie, E. Strauss, J. Arino, Moonlighting proteins Hal3 and Vhs3 form a heteromeric PPCDC with Ykl088w in yeast CoA biosynthesis, Nat. Chem. Biol. 5 (2009) 920–928. https://doi.org/10.1038/nchembio.243.

[18] J. Clotet, F. Posas, E. De Nadal, J. Arino, The NH2-terminal extension of protein phosphatase PPZ1 has an essential functional role, J. Biol. Chem. 271 (1996) 26349–26355. https://doi.org/10.1074/jbc.271.42.26349.

[19] J. Clotet, E. Garí, M. Aldea, J. Ariño, The Yeast Ser/Thr Phosphatases Sit4 and Ppz1 Play Opposite Roles in Regulation of the Cell Cycle, Mol. Cell. Biol. 19 (1999) 2408–2415. https://doi.org/10.1128/MCB.19.3.2408.

[20] L.F. Stevenson, B.K. Kennedy, E. Harlow, A large-scale overexpression screen in Saccharomyces cerevisiae identifies previously uncharacterized cell cycle genes, Proc. Natl. Acad. Sci. 98 (2001) 3946–3951. https://doi.org/10.1073/pnas.051013498.

[21] K. Makanae, R. Kintaka, T. Makino, H. Kitano, H. Moriya, Identification of dosage-sensitive genes in Saccharomyces cerevisiae using the genetic tug-of-war method., Genome Res. 23 (2013) 300–11. https://doi.org/10.1101/gr.146662.112.

[22] A. Adams, D.E. Gottschling, C.A. Kaiser, T. Stearns, Methods in yeast genetics : a Cold Spring Harbor Laboratory course manual, Cold Spring Harbor Laboratory Press, 1998.

[23] M. Marquina, E. Queralt, A. Casamayor, J. Ariño, Lack of the Glc7 phosphatase regulatory subunit Ypi1 activates the morphogenetic checkpoint, Int. J. Biochem. Cell Biol. 44 (2012) 1862–1871. https://doi.org/10.1016/j.biocel.2012.06.029.

[24] M.R. Green, J. Sambrook, Molecular Cloning: A laboratory Manual., 4th ed., Cold Spring Harbor Laboratory Press, NY, New York, 2012. http://www.molecularcloning.com/.

[25] M.S. Longtine, A. Mckenzie III, D.J. Demarini, N.G. Shah, A. Wach, A. Brachat, P. Philippsen, J.R. Pringle, Additional modules for versatile and economical PCR-based gene deletion and modification in Saccharomyces cerevisiae, Yeast. 14 (1998) 953–961. https://doi.org/10.1002/(SICI)1097-0061(199807)14:10<953::AID-YEA293>3.0.CO;2-U.

[26] G. Bellí, E. Garí, M. Aldea, E. Herrero, Functional analysis of yeast essential genes using a promoter-substitution cassette and the tetracycline-regulatable dual expression system., Yeast. 14 (1998) 1127–38. https://doi.org/10.1002/(SICI)1097-0061(19980915)14:12<1127::AID-YEA300>3.0.CO;2-#.

[27] E.A. Winzeler, D.D. Shoemaker, A. Astromoff, H. Liang, K. Anderson, B. Andre, R. Bangham, R. Benito, J.D. Boeke, H. Bussey, A.M. Chu, C. Connelly, K. Davis, F. Dietrich, S.W. Dow, M. El Bakkoury, F. Foury, S.H. Friend, E. Gentalen, G. Giaever, J.H. Hegemann, T. Jones, M. Laub, H. Liao, N. Liebundguth, D.J. Lockhart, A. Lucau-Danila, M. Lussier, N. M'Rabet, P. Menard, M. Mittmann, C. Pai, C. Rebischung, J.L. Revuelta, L. Riles, C.J. Roberts, P. Ross-MacDonald, B. Scherens, M. Snyder, S. Sookhai-Mahadeo, R.K. Storms, S. Véronneau, M. Voet, G. Volckaert, T.R. Ward, R. Wysocki, G.S. Yen, K. Yu, K. Zimmermann, P. Philippsen, M. Johnston, R.W. Davis, Functional characterization of the S. cerevisiae genome by gene deletion and parallel analysis., Science. 285 (1999) 901–6. https://doi.org/10.1126/science.285.5429.901.

[28] E. Garí, L. Piedrafita, M. Aldea, E. Herrero, A set of vectors with a tetracycline-regulatable promoter system for modulated gene expression in Saccharomyces cerevisiae., Yeast. 13 (1997) 837–48. https://doi.org/10.1002/(SICI)1097-0061(199707)13:9<837::AID-YEA145>3.0.CO;2-T.

[29] A. Shevchenko, H. Tomas, J. Havliš, J. V. Olsen, M. Mann, In-gel digestion for mass spectrometric characterization of proteins and proteomes, Nat. Protoc. 1 (2007) 2856–2860. https://doi.org/10.1038/nprot.2006.468.

[30] D. Kressler, J. de la Cruz, M. Rojo, P. Linder, Fal1p is an essential DEAD-box protein involved in 40S-ribosomal-subunit biogenesis in Saccharomyces cerevisiae., Mol. Cell. Biol. 17 (1997) 7283–94. https://doi.org/10.1128/mcb.17.12.7283.

[31] A. Ferrando, S.J. Kron, G. Rios, G.R. Fink, R. Serrano, Regulation of cation transport in Saccharomyces cerevisiae by the salt tolerance gene HAL3, Mol. Cell Biol. 15 (1995) 5470–5481. https://doi.org/10.1128/mcb.15.10.5470.

[32] G. Dieci, L. Bottarelli, S. Ottonello, A General Procedure for the Production of Antibody Reagents Against Eukaryotic Ribosomal Proteins, Protein Pept. Lett. 12 (2005) 555–560. https://doi.org/10.2174/0929866054395860.

[33] M.A. Collart, S. Oliviero, Preparation of Yeast RNA, in: Curr. Protoc. Mol. Biol., John Wiley & Sons, Ltd, 1993: pp. 13.12.1-13.12.5. https://doi.org/10.1002/0471142727.mb1312s23.

[34] D. Kressler, J. de la Cruz, M. Rojo, P. Linder, Dbp6p is an essential putative ATP-dependent RNA helicase required for 60S-ribosomal-subunit assembly in Saccharomyces cerevisiae., Mol. Cell. Biol. 18 (1998) 1855–65. https://doi.org/10.1128/mcb.18.4.1855.

[35] J. Venema, R.J. Planta, H.A. Raué, In Vivo Mutational Analysis of Ribosomal RNA in Saccharomyces cerevisiae, in: Protein Synth., Humana Press, New Jersey, 1998: pp. 257–270. https://doi.org/10.1385/0-89603-397-X:257.

[36] J.M. Park, H.S. Kim, S.J. Han, M.S. Hwang, Y.C. Lee, Y.J. Kim, In vivo requirement of activator-specific binding targets of mediator., Mol. Cell. Biol. 20 (2000) 8709–19. https://doi.org/10.1128/mcb.20.23.8709-8719.2000.

[37] Z. Liu, L.C. Myers, Fungal mediator tail subunits contain classical transcriptional activation domains., Mol. Cell. Biol. 35 (2015) 1363–75. https://doi.org/10.1128/MCB.01508-14.

[38] J.I. Piruat, S. Chávez, A. Aguilera, The yeast HRS1 gene is involved in positive and negative regulation of transcription and shows genetic characteristics similar to SIN4 and GAL11., Genetics. 147 (1997) 1585–94. http://www.ncbi.nlm.nih.gov/pubmed/9409823 (accessed February 6, 2019).

[39] H. Kubota, K. Ota, Y. Sakaki, T. Ito, Budding Yeast GCN1 Binds the GI Domain to Activate the eIF2α Kinase GCN2, J. Biol. Chem. 276 (2001) 17591–17596. https://doi.org/10.1074/jbc.M011793200.

[40] G.P. Cosentino, T. Schmelzle, A. Haghighat, S.B. Helliwell, M.N. Hall, N.

Sonenberg, Eap1p, a novel eukaryotic translation initiation factor 4E-associated protein in Saccharomyces cerevisiae., Mol. Cell. Biol. 20 (2000) 4604–13. https://doi.org/10.1128/mcb.20.13.4604-4613.2000.

[41] M. Altmann, N. Schmitz, C. Berset, H. Trachsel, A novel inhibitor of cap-dependent translation initiation in yeast: p20 competes with eIF4G for binding to eIF4E, EMBO J. 16 (1997) 1114–1121. https://doi.org/10.1093/emboj/16.5.1114.

[42] J. de la Cruz, I. Iost, D. Kressler, P. Linder, The p20 and Ded1 proteins have antagonistic roles in eIF4E-dependent translation in Saccharomyces cerevisiae, Proc. Natl. Acad. Sci. 94 (1997) 5201–5206. https://doi.org/10.1073/pnas.94.10.5201.

[43] C. Adam, E. Erdei, C. Casado, L. Kovacs, A. Gonzalez, L. Majoros, K. Petrenyi, P. Bagossi, I. Farkas, M. Molnar, I. Pocsi, J. Arino, V. Dombradi, Protein phosphatase CaPpz1 is involved in cation homeostasis, cell wall integrity and virulence of Candida albicans, Microbiology. 158 (2012) 1258–1267. https://doi.org/10.1099/mic.0.057075-0.

[44] E. Chen, M.S. Choy, K. Petrényi, Z. Kónya, F. Erdődi, V. Dombrádi, W. Peti, R. Page, Molecular Insights into the Fungus-Specific Serine/Threonine Protein Phosphatase Z1 in Candida albicans., MBio. 7 (2016). https://doi.org/10.1128/mBio.00872-16.

[45] C. Molero, C. Casado, J. Ariño, The inhibitory mechanism of Hal3 on the yeast Ppz1 phosphatase: A mutagenesis analysis., Sci. Rep. 7 (2017) 8819. https://doi.org/10.1038/s41598-017-09360-5.

[46] I. Munoz, A. Ruiz, M. Marquina, A. Barcelo, A. Albert, J. Arino, Functional characterization of the yeast Ppz1 phosphatase inhibitory subunit Hal3: a mutagenesis study, J.Biol.Chem. 279 (2004) 42619–42627. https://doi.org/10.1074/jbc.M405656200.

[47] J.F. Cannon, Function of protein phosphatase-1, Glc7, in Saccharomyces cerevisiae., Adv. Appl. Microbiol. 73 (2010) 27–59. https://doi.org/10.1016/S0065-2164(10)73002-1.

[48] Z. Yin, S. Wilson, N.C. Hauser, H. Tournu, J.D. Hoheisel, A.J.P. Brown, Glucose triggers different global responses in yeast, depending on the strength of the signal, and transiently stabilizes ribosomal protein mRNAs., Mol. Microbiol. 48 (2003) 713–24. https://doi.org/10.1046/j.1365-2958.2003.03478.x.

[49] J. Urban, A. Soulard, A. Huber, S. Lippman, D. Mukhopadhyay, O. Deloche, V. Wanke, D. Anrather, G. Ammerer, H. Riezman, J.R. Broach, C. De Virgilio, M.N. Hall, R. Loewith, Sch9 is a major target of TORC1 in Saccharomyces cerevisiae., Mol. Cell. 26 (2007) 663–74. https://doi.org/10.1016/j.molcel.2007.04.020.

[50] M.-A. Deprez, E. Eskes, T. Wilms, P. Ludovico, J. Winderickx, pH homeostasis links the nutrient sensing PKA/TORC1/Sch9 ménage-à-trois to stress tolerance and longevity., Microb. Cell (Graz, Austria). 5 (2018) 119–136. https://doi.org/10.15698/mic2018.03.618.

[51] R. Oughtred, C. Stark, B.-J. Breitkreutz, J. Rust, L. Boucher, C. Chang, N. Kolas, L. O'Donnell, G. Leung, R. McAdam, F. Zhang, S. Dolma, A. Willems, J. Coulombe-Huntington, A. Chatr-aryamontri, K. Dolinski, M. Tyers, The BioGRID interaction database: 2019 update, Nucleic Acids Res. 47 (2019) D529–D541. https://doi.org/10.1093/nar/gky1079.

[52] B. Márkus, K. Szabó, W.P. Pfliegler, K. Petrényi, E. Boros, I. Pócsi, J. Tőzsér, É. Csősz, V. Dombrádi, Proteomic analysis of protein phosphatase Z1 from Candida albicans, PLoS One. 12 (2017) e0183176. https://doi.org/10.1371/journal.pone.0183176.

[53] R. Coppolecchia, P. Buser, A. Stotz, P. Linder, A new yeast translation initiation factor suppresses a mutation in the eIF-4A RNA helicase., EMBO J. 12 (1993) 4005–11. http://www.ncbi.nlm.nih.gov/pubmed/8404866 (accessed January 23, 2020).

[54] S. Anda, R. Zach, B. Grallert, Activation of Gcn2 in response to different stresses, PLoS One. 12 (2017) e0182143. https://doi.org/10.1371/journal.pone.0182143.

[55] C.E. Simpson, M.P. Ashe, Adaptation to stress in yeast: To translate or not?, Biochem. Soc. Trans. 40 (2012) 794–799. https://doi.org/10.1042/BST20120078.

[56] R.A. Crawford, G.D. Pavitt, Translational regulation in response to stress in *Saccharomyces cerevisiae*, Yeast. 36 (2019) 5–21. https://doi.org/10.1002/yea.3349.

[57] R.C. Wek, J.F. Cannon, T.E. Dever, A.G. Hinnebusch, Truncated protein phosphatase GLC7 restores translational activation of GCN4 expression in yeast mutants defective for the eIF-2 alpha kinase GCN2., Mol. Cell. Biol. 12 (1992) 5700–10. https://doi.org/10.1128/mcb.12.12.5700.

[58] M. Rojas, A.-C. Gingras, T.E. Dever, Protein phosphatase PP1/GLC7 interaction domain in yeast eIF2γ bypasses targeting subunit requirement for eIF2α dephosphorylation., Proc. Natl. Acad. Sci. U. S. A. 111 (2014) E1344-53. https://doi.org/10.1073/pnas.1400129111.

[59] M. Garcia-Barrio, J. Dong, V.A. Cherkasova, X. Zhang, F. Zhang, S. Ufano, R. Lai, J. Qin, A.G. Hinnebusch, Serine 577 is phosphorylated and negatively affects the tRNA binding and eIF2alpha kinase activities of GCN2., J. Biol. Chem. 277 (2002) 30675–83. https://doi.org/10.1074/jbc.M203187200.

[60] M. Costanzo, A. Baryshnikova, J. Bellay, Y. Kim, E.D. Spear, C.S. Sevier, H. Ding,

J.L.Y. Koh, K. Toufighi, S. Mostafavi, J. Prinz, R.P. St. Onge, B. Vandersluis, T. Makhnevych, F.J. Vizeacoumar, S. Alizadeh, S. Bahr, R.L. Brost, Y. Chen, M. Cokol, R. Deshpande, Z. Li, Z.Y. Lin, W. Liang, M. Marback, J. Paw, B.J.S. Luis, E. Shuteriqi, A.H.Y. Tong, N. Van Dyk, I.M. Wallace, J.A. Whitney, M.T. Weirauch, G. Zhong, H. Zhu, W.A. Houry, M. Brudno, S. Ragibizadeh, B. Papp, C. Pál, F.P. Roth, G. Giaever, C. Nislow, O.G. Troyanskaya, H. Bussey, G.D. Bader, A.C. Gingras, Q.D. Morris, P.M. Kim, C.A. Kaiser, C.L. Myers, B.J. Andrews, C. Boone, The genetic landscape of a cell, Science (80-.). 327 (2010) 425–431. https://doi.org/10.1126/science.1180823.

[61] M. Costanzo, B. VanderSluis, E.N. Koch, A. Baryshnikova, C. Pons, G. Tan, W. Wang, M.M.M.M. Usaj, J. Hanchard, S.D. Lee, V. Pelechano, E.B. Styles, M. Billmann, J. van Leeuwen, N. Van Dyk, Z.-Y.Z.Y. Lin, E. Kuzmin, J. Nelson, J.S. Piotrowski, T. Srikumar, S. Bahr, Y. Chen, R. Deshpande, C.F. Kurat, S.C. Li, Z. Li, M.M.M.M. Usaj, H. Okada, N. Pascoe, B.-J. San Luis, S. Sharifpoor, E. Shuteriqi, S.W. Simpkins, J. Snider, H.G. Suresh, Y. Tan, H. Zhu, N. Malod-Dognin, V. Janjic, N. Przulj, O.G. Troyanskaya, I. Stagljar, T. Xia, Y. Ohya, A.C.A.-C. Gingras, B. Raught, M. Boutros, L.M. Steinmetz, C.L. Moore, A.P. Rosebrock, A.A. Caudy, C.L. Myers, B. Andrews, C. Boone, B.J.S. Luis, S. Sharifpoor, E. Shuteriqi, S.W. Simpkins, J. Snider, H.G. Suresh, Y. Tan, H. Zhu, N. Malod-Dognin, V. Janjic, N. Przulj, O.G. Troyanskaya, I. Stagljar, T. Xia, Y. Ohya, A.C.A.-C. Gingras, B. Raught, M. Boutros, L.M. Steinmetz, C.L. Moore, A.P. Rosebrock, A.A. Caudy, C.L. Myers, B. Andrews, C. Boone, A global genetic interaction network maps a wiring diagram of cellular function, Science (80-.). 353 (2016) aaf1420–aaf1420. https://doi.org/10.1126/science.aaf1420.

[62] S. Sharifpoor, D. van Dyk, M. Costanzo, A. Baryshnikova, H. Friesen, A.C. Douglas, J.-Y. Youn, B. VanderSluis, C.L. Myers, B. Papp, C. Boone, B.J. Andrews, Functional wiring of the yeast kinome revealed by global analysis of genetic network motifs., Genome Res. 22 (2012) 791–801. https://doi.org/10.1101/gr.129213.111.

[63] E. de Nadal, R.P. Fadden, A. Ruiz, T. Haystead, J. Ariño, A Role for the Ppz Ser/Thr Protein Phosphatases in the Regulation of Translation Elongation Factor 1Bα, J. Biol. Chem. 276 (2001) 14829–14834. https://doi.org/10.1074/jbc.M010824200.

[64] Larasati, B. Duncker, Mechanisms Governing DDK Regulation of the Initiation of DNA Replication, Genes (Basel). 8 (2016) 3. https://doi.org/10.3390/genes8010003.

[65] G.M. Venturi, A. Bloecher, T. Williams-Hart, K. Tatchell, Genetic interactions

between GLC7, PPZ1 and PPZ2 in saccharomyces cerevisiae., Genetics. 155 (2000) 69–83. http://www.ncbi.nlm.nih.gov/pubmed/10790385.

[66] M.A. Garcia-Gimeno, I. Munoz, J. Arino, P. Sanz, Molecular characterization of Ypi1, a novel Saccharomyces cerevisiae type 1 protein phosphatase inhibitor, J. Biol. Chem. 278 (2003) 47744–47752. https://doi.org/10.1074/jbc.M306157200.

[67] H. Liu, J. Krizek, A. Bretscher, Construction of a GAL1-regulated yeast cDNA expression library and its application to the identification of genes whose overexpression causes lethality in yeast., Genetics. 132 (1992) 665–73. http://www.ncbi.nlm.nih.gov/pubmed/1468625.

[68] A. Ghosh, J.F. Cannon, Analysis of protein phosphatase-1 and aurora protein kinase suppressors reveals new aspects of regulatory protein function in Saccharomyces cerevisiae., PLoS One. 8 (2013) e69133. https://doi.org/10.1371/journal.pone.0069133.

[69] B.A. Pinsky, C.R. Nelson, S. Biggins, Protein phosphatase 1 regulates exit from the spindle checkpoint in budding yeast., Curr. Biol. 19 (2009) 1182–7. https://doi.org/10.1016/j.cub.2009.06.043.

[70] S. Black, P.D. Andrews, A.A. Sneddon, M.J.R. Stark, A regulatedMET3-GLC7 gene fusion provides evidence of a mitotic role forSaccharomyces cerevisiae protein phosphatase 1, Yeast. 11 (1995) 747–759. https://doi.org/10.1002/yea.320110806.

[71] S. Zhang, S. Guha, F.C. Volkert, The Saccharomyces SHP1 gene, which encodes a regulator of phosphoprotein phosphatase 1 with differential effects on glycogen metabolism, meiotic differentiation, and mitotic cell cycle progression., Mol. Cell. Biol. 15 (1995) 2037–2050. https://doi.org/10.1128/MCB.15.4.2037.

[72] S. Duffy, H.K. Fam, Y.K. Wang, E.B. Styles, J.-H. Kim, J.S. Ang, T. Singh, V. Larionov, S.P. Shah, B. Andrews, C.F. Boerkoel, P. Hieter, Overexpression screens identify conserved dosage chromosome instability genes in yeast and human cancer., Proc. Natl. Acad. Sci. U. S. A. 113 (2016) 9967–76. https://doi.org/10.1073/pnas.1611839113.

[73] J. Zhu, D. Heinecke, W.A. Mulla, W.D. Bradford, B. Rubinstein, A. Box, J.S. Haug, R. Li, Single-Cell Based Quantitative Assay of Chromosome Transmission Fidelity., G3 (Bethesda). 5 (2015) 1043–56. https://doi.org/10.1534/g3.115.017913.

[74] C.B. Brachmann, A. Davies, G.J. Cost, E. Caputo, J. Li, P. Hieter, J.D. Boeke, Designer deletion strains derived from Saccharomyces cerevisiae S288C: A useful set of strains and plasmids for PCR-mediated gene disruption and other applications, Yeast. 14 (1998) 115–132. https://doi.org/10.1002/(SICI)1097-

0061(19980130)14:2<115::AID-YEA204>3.0.CO;2-2.

[75] A.G. Cridge, L.M. Castelli, J.B. Smirnova, J.N. Selley, W. Rowe, S.J. Hubbard, J.E.G. McCarthy, M.P. Ashe, C.M. Grant, G.D. Pavitt, Identifying eIF4E-binding protein translationally-controlled transcripts reveals links to mRNAs bound by specific PUF proteins., Nucleic Acids Res. 38 (2010) 8039–50. https://doi.org/10.1093/nar/gkq686.

[76] J.M. Cherry, E.L. Hong, C. Amundsen, R. Balakrishnan, G. Binkley, E.T. Chan, K.R. Christie, M.C. Costanzo, S.S. Dwight, S.R. Engel, D.G. Fisk, J.E. Hirschman, B.C. Hitz, K. Karra, C.J. Krieger, S.R. Miyasato, R.S. Nash, J. Park, M.S. Skrzypek, M. Simison, S. Weng, E.D. Wong, Saccharomyces Genome Database: The genomics resource of budding yeast, Nucleic Acids Res. 40 (2012). https://doi.org/10.1093/nar/gkr1029.

[77] P. Shannon, A. Markiel, O. Ozier, N.S. Baliga, J.T. Wang, D. Ramage, N. Amin, B. Schwikowski, T. Ideker, Cytoscape: A Software Environment for Integrated Models of Biomolecular Interaction Networks, Genome Res. 13 (2003) 2498–2504. https://doi.org/10.1101/gr.1239303.

Figure legends

Figure 1.- Characterization of the Ppz1-overexpressing strain ZCZ01. A) Wild-type (WT) and ZCZ01 (*GAL1-10:PPZ1*) cells were grown on YP with 2% raffinose (YP-Raff) and 2% galactose was added. Samples were taken at the indicated times, electrophoresed and immunoblotted using polyclonal anti-Ppz1 antibodies. Ponceau staining is shown for loading and transfer reference. Wild-type and ZCZ01 samples were loaded in the same gel and are shown separated for illustrative purposes. B) Top panel. Strains were grown on YP-Raff and the indicated amounts of galactose were added. Incubation was resumed for 20 h and Ppz1 detected by immunoblot as above. Bottom panel. Wild-type BY4741 (open bars) and ZCZ01 (closed bars) cells grown on YP-Raff were diluted to OD_{600}=0.04, the indicated amounts of galactose were added, and growth was resumed for 24 h. Data are mean ± SEM from three experiments made by triplicate. C) Cells were collected after the indicated times of addition of 2% galactose (+), stained with propidium iodine and the DNA content evaluated by flow cytometry. The arrow denotes the absence of 2C peak in Ppz1 overexpressing cells. D) Wild-type BY4741 (open bars) and ZCZ01 (closed bars) were grown for 20 h in YP-Raff in the presence of 2% galactose (Gal). After centrifugation, cells were resuspended in YP-Raff and diverse dilutions plated on YP plates with the indicated carbon sources (Glu, glucose). Colonies were counted after 3 days. Wild-type was considered as 100% viability. Data correspond to the mean ± SEM from six experiments.

Figure 2.- Toxicity of Ppz1 overexpression is due to increased phosphatase activity. A) Upper panel. The indicated strains were transformed with pYES2-based plasmids, which express wild-type Ppz1 or catalytic inactive $Ppz1^{R451L}$ from the *GAL1-10* promoter, and spotted at OD_{600}=0.05 (plus 1/5 dilutions) on synthetic medium lacking uracil with 2% glucose (Glu) or 2% galactose (Gal) as carbon source. Ø, empty plasmid. Pictures were taken after 4 days of growth. Lower panel. Protein extracts (25 µg) of the strains used in the upper panel were electrophoresed, transferred to membranes and probed with anti-Ppz1 antibodies. Ponceau staining of the membrane is included as loading and transfer

control. B) Strains were transformed with the indicated plasmids (YEplac195-based for Hal3 and Vhs3; pRS699 for HsHal3, encoding human PPCDC [17]) and spotted as in panel A. Growth was monitored after 2 days.

Figure 3.- Chromosomal expression of Ppz1 from *tetO*-regulatable promoters. A) Wild-type BY4741 and its MLM03 and MLM04 derivatives (*tetO*$_2$ and *tetO*$_7$, respectively) were transformed with YEp195-based vectors and grown on synthetic medium lacking uracil in the presence of doxycycline (100 µg/ml). Cells were resuspended in the same medium lacking doxycycline, grown for 5 h, and dilutions were spotted on synthetic plates lacking uracil in the presence (+ DOX) or the absence of doxycycline (-DOX), and containing the indicated carbon sources. Pictures were taken after 3 days of incubation. B) BY4741 cells (WT) and its *ppz1* and MLM04 derivatives were grown as indicated in Material and Methods and protein extracts prepared at the indicated times after removal of doxycycline. Samples (40 µg of protein) were electrophoresed and transferred to membranes. Membranes were probed with anti-Ppz1 and anti-Hal3 antibodies.

Figure 4.- High-copy number suppressors of the growth defect of MLM04 cells. A) The indicated genes, isolated in the high-copy suppressor screen, were cloned in plasmid YEplac195 and introduced in strain MLM04. Cultures were spotted as in Fig. 2A and pictures taken after 3 days (the *HAL3* gene is included as a control). B) Growth of strains carrying a combination of selected suppressors in the absence of doxycycline and in the presence of 0.25% glucose (3 days) or 2% galactose (6 days) as carbon source. C) The interaction network between the different suppressors when cells are grown on 0.25% glucose or 2% galactose (data taken from Table S4 and S5) was visualized with the Cytoscape (v. 3.7.2) software [77]. Color of nodes define functional categories of the genes (blue, ribosomal biogenesis; green, sporulation; red, ribosomal proteins), and edge colors indicate the intensity of the interaction determined as the difference between the growth of the strain carrying the most potent suppressor in the specific gene pair and the strain carrying both genes. The included color scale ranges from 0.5 (very weak effect) to 5 (full growth recovery, as that produced by the *HAL3* gene).

Figure 5.- Ppz1 associates with ribosomal fractions and its overexpression causes polysome depletion. A) Protein extracts were prepared from BY4741 cells harboring pEGH plasmids expressing GST or an inactive GST-Ppz1^{R451L} version and shifted for 60 min to 2% galactose. After SDS-PAGE (10% acrylamide), gels were stained with Coomassie Blue and diverse slices containing apparent GST-Ppz1 specific bands (denoted in the gel by "I" and Roman numerals) were excised. Equivalent regions were also sliced from control (GST) lanes. Samples were processed and trypsinized proteins were identified by mass spectrometry. Three independent experiments were performed, and a representative stained gel is shown. B) Normalized profiles of fractionated ribosomal components from strains BY4741 and MLM04 carrying an empty episomal plasmid, and MLM04 cells bearing *HAL3* in high-copy number. Numbers denote the P/M (polysome/monosome ratio) calculated from three experiments (mean ± SEM). C) BY4741 cells transformed with an empty pCM190 plasmid were grown and extracts prepared and electrophoresed. Endogenous Ppz1 (ePpz1) was detected by immunoblot. Whole extracts from BY4741 (WT) and the *ppz1* mutant are included for reference. Immunodetection of Rps8 and Rpl14, as markers of the 40S and 60S ribosomal subunits, respectively, is also shown. D) The indicated fractions from the rightmost strain (MLM04 + YEp195-*HAL3*) were electrophoresed, transferred to membranes and probed with anti-Ppz1 and anti-Hal3 antibodies. Whole extracts from BY4741 (WT) and the *hal3* mutant are included for reference.

Figure 6.- Overexpression of Ppz1 increases phosphorylation of eIF2α at Ser-51. A) Strain BY4741 (WT) and ZCZ01 were grown on raffinose and Ppz1 expression induced by addition of galactose (2%). Protein extracts (40 μg of protein) were prepared at the indicated times after induction and electrophoresed. The levels of Ppz1 were determined with an anti-Ppz1 antibody and the phosphorylation state of eIF2α was monitored with an antibody that recognizes the protein when phosphorylated at Ser-51 (mAb #3597, Cell Signaling). B) Strain BY4741 and its isogenic *gcn2*Δ derivative were transformed with the empty pYES2 vector and the same vector expressing Ppz1; cultures were processed as above for determination of Ppz1 content and eIF2α phosphorylation status. C) Strain BY4741 and its isogenic *gcn2*Δ derivative were transformed with the

indicated plasmids (expressing *PPZ1* at different levels, from pCM188, the lowest, to pCM190, the highest). Cells were spotted in the presence or absence of doxycycline on synthetic medium plates lacking uracil and with the indicated concentrations of glucose. Pictures were taken after 6 days of incubation.

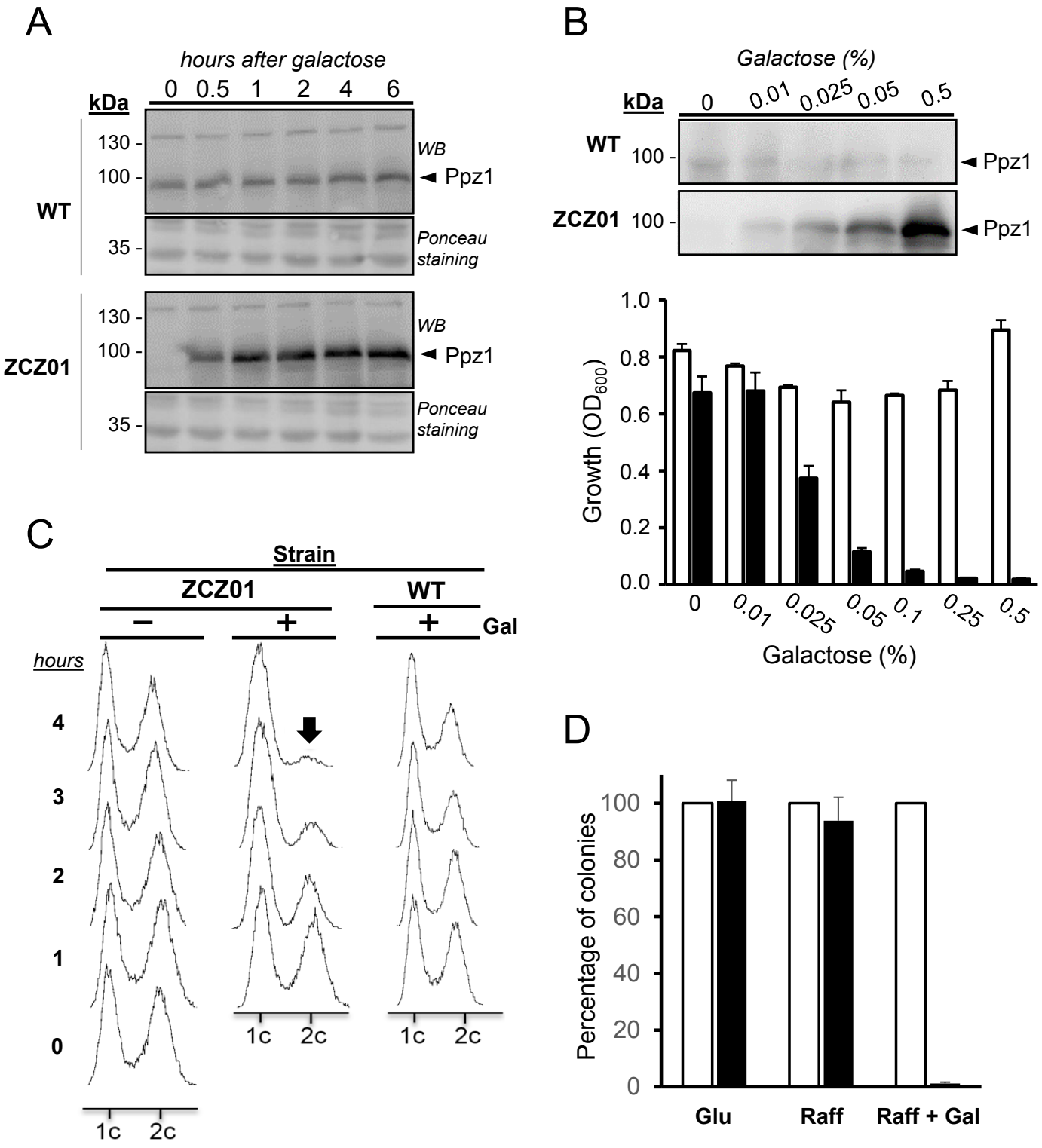
A
hours after galactose
0 0.5 1 2 4 6
kDa
130 -
100 -
WT
WB
Ppz1
35 -
Ponceau staining
ZCZ01
B
Galactose (%)
0 0.01 0.025 0.05 0.5
Growth (OD600)
1.0
0.8
0.6
0.4
0.2
0.0
0 0.01 0.025 0.05 0.1 0.25 0.5
Galactose (%)
C
Strain
ZCZ01
WT
Gal
hours
4
3
2
1
0
1c 2c
D
Percentage of colonies
100
80
60
40
20
0
Glu
Raff
Raff + Gal

Figure 1

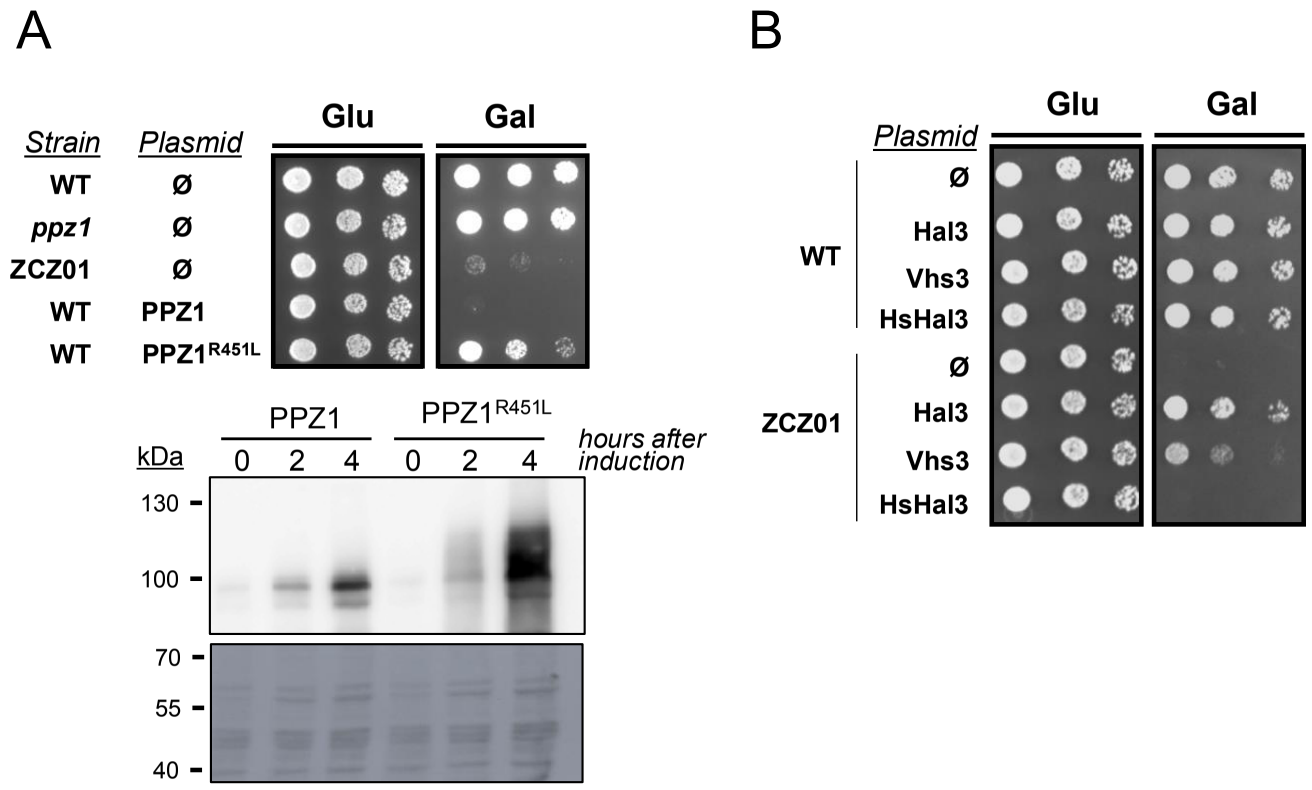
A
Strain
Plasmid
Glu
Gal
WT
Ø
ppz1
Ø
ZCZ01
Ø
WT
PPZ1
WT
PPZ1R451L
PPZ1
PPZ1R451L
kDa
0 2 4 0 2 4
hours after induction
130
100
70
55
40
B
Glu
Gal
Plasmid
WT
Ø
Hal3
Vhs3
HsHal3
ZCZ01
Ø
Hal3
Vhs3
HsHal3

Fig. 2

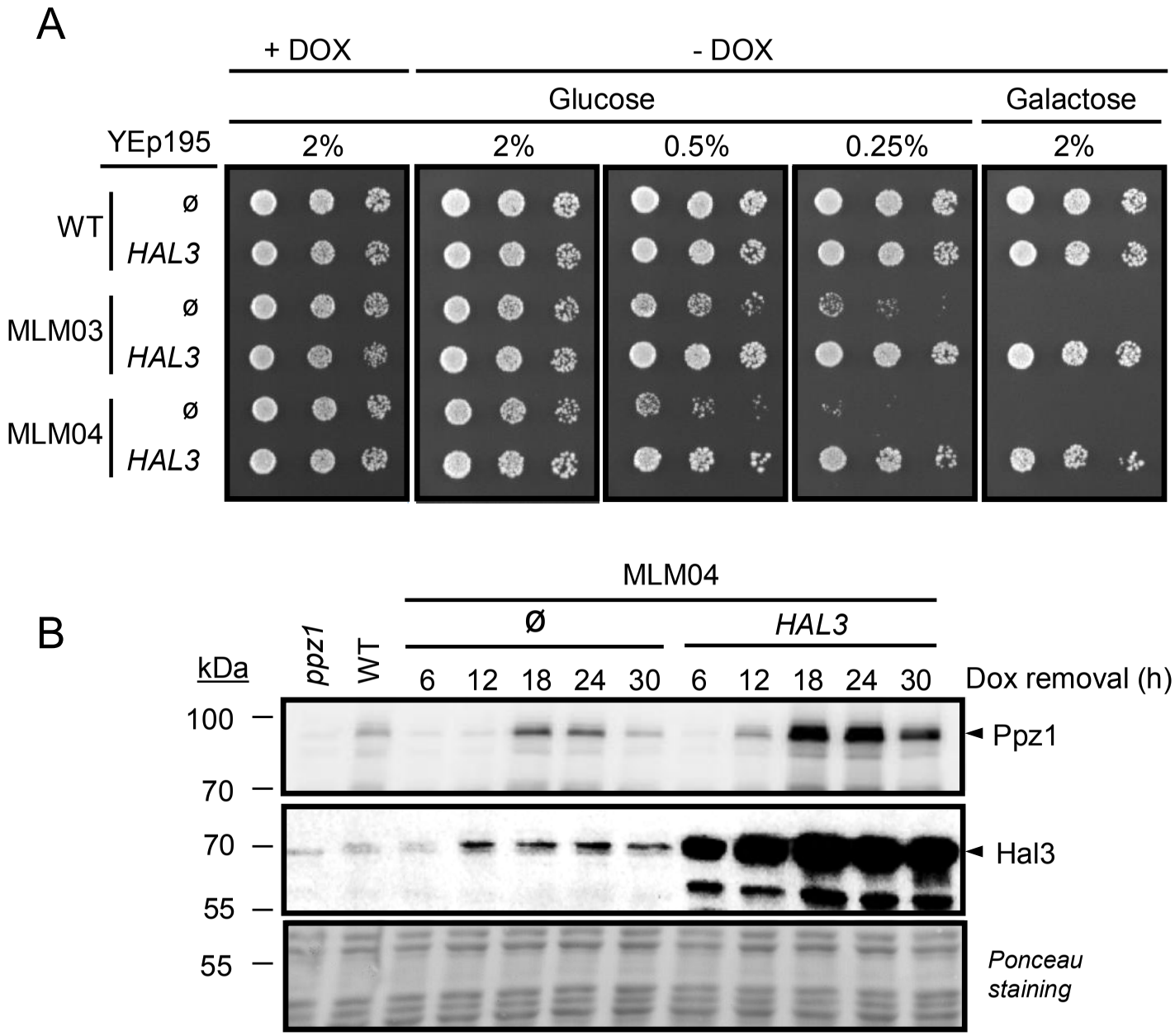
A
+ DOX
- DOX
Glucose
Galactose
YEp195
2%
2%
0.5%
0.25%
2%
WT
ø
HAL3
MLM03
ø
HAL3
MLM04
ø
HAL3
B
MLM04
ø
HAL3
kDa
ppz1
WT
6 12 18 24 30 6 12 18 24 30
Dox removal (h)
100
70
Ppz1
70
55
Hal3
55
Ponceau staining

Fig. 3

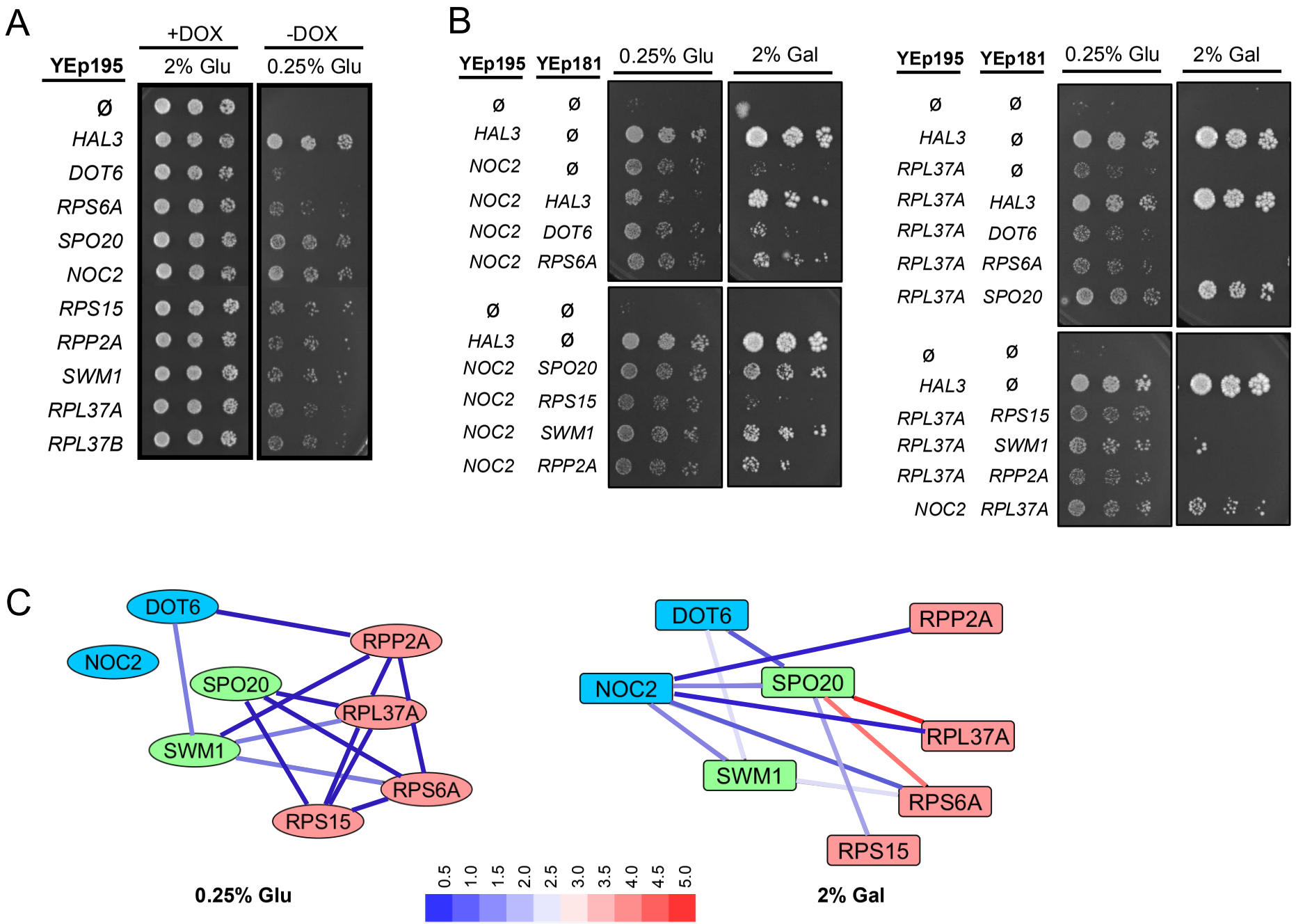
A
+DOX
-DOX
YEp195
2% Glu
0.25% Glu
Ø
HAL3
DOT6
RPS6A
SPO20
NOC2
RPS15
RPP2A
SWM1
RPL37A
RPL37B
B
YEp195
YEp181
0.25% Glu
2% Gal
Ø Ø
HAL3 Ø
NOC2 Ø
NOC2 HAL3
NOC2 DOT6
NOC2 RPS6A
Ø Ø
HAL3 Ø
NOC2 SPO20
NOC2 RPS15
NOC2 SWM1
NOC2 RPP2A
YEp195
YEp181
0.25% Glu
2% Gal
Ø Ø
HAL3 Ø
RPL37A Ø
RPL37A HAL3
RPL37A DOT6
RPL37A RPS6A
RPL37A SPO20
Ø Ø
HAL3 Ø
RPL37A RPS15
RPL37A SWM1
RPL37A RPP2A
NOC2 RPL37A
C
DOT6
RPP2A
NOC2
SPO20
RPL37A
SWM1
RPS6A
RPS15
0.25% Glu
0.5 1.0 1.5 2.0 2.5 3.0 3.5 4.0 4.5 5.0
DOT6
RPP2A
NOC2
SPO20
RPL37A
SWM1
RPS6A
RPS15
2% Gal

Fig. 4

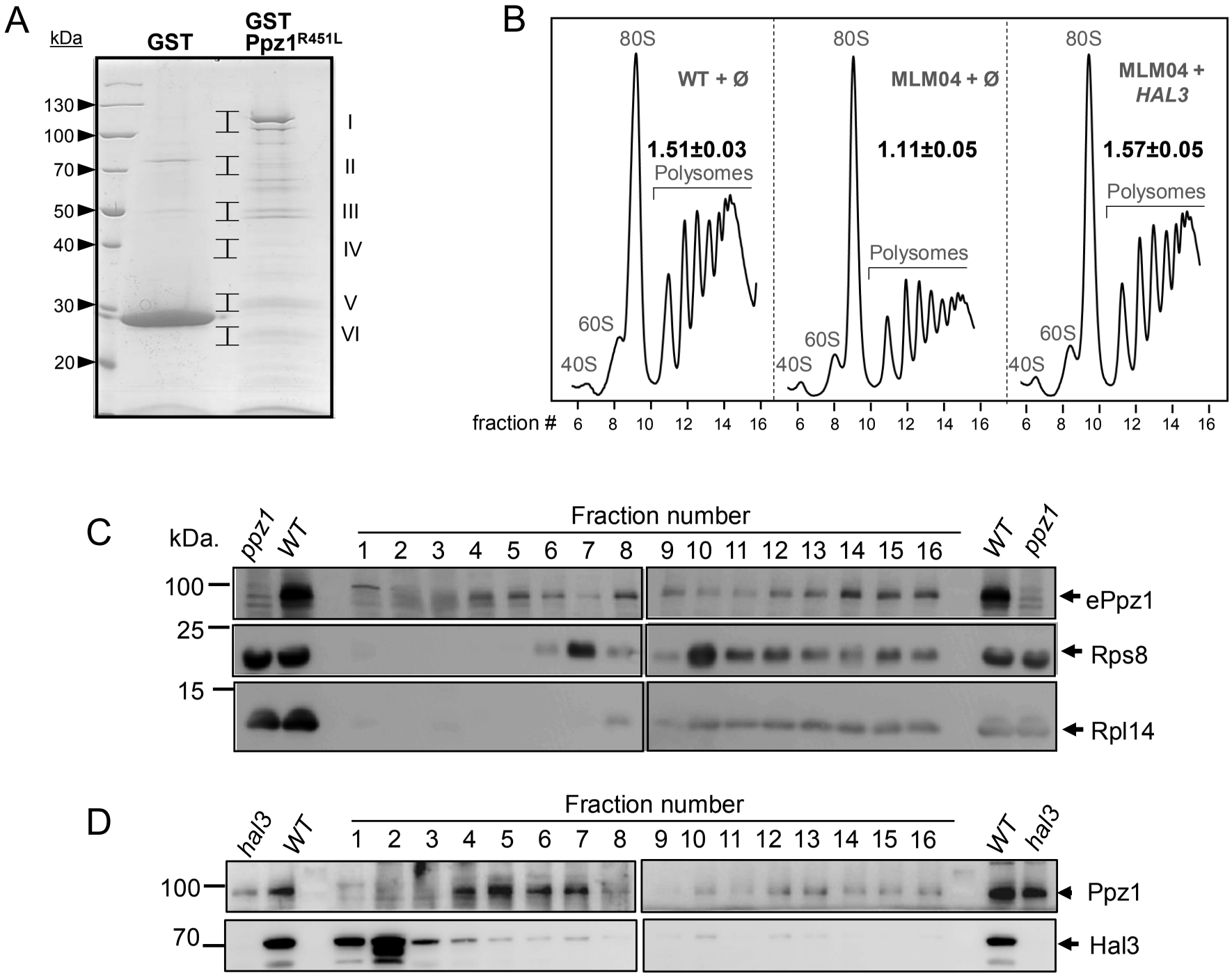
A
kDa
GST
GST Ppz1R451L
130
100
70
50
40
30
20
I
II
III
IV
V
VI
B
80S
WT + Ø
1.51±0.03
Polysomes
60S
40S
MLM04 + Ø
1.11±0.05
MLM04 + HAL3
1.57±0.05
fraction #
6 8 10 12 14 16
C
kDa.
ppz1
WT
Fraction number
1 2 3 4 5 6 7 8 9 10 11 12 13 14 15 16
100
25
15
ePpz1
Rps8
Rpl14
D
hal3
Ppz1
Hal3
70

Fig. 5

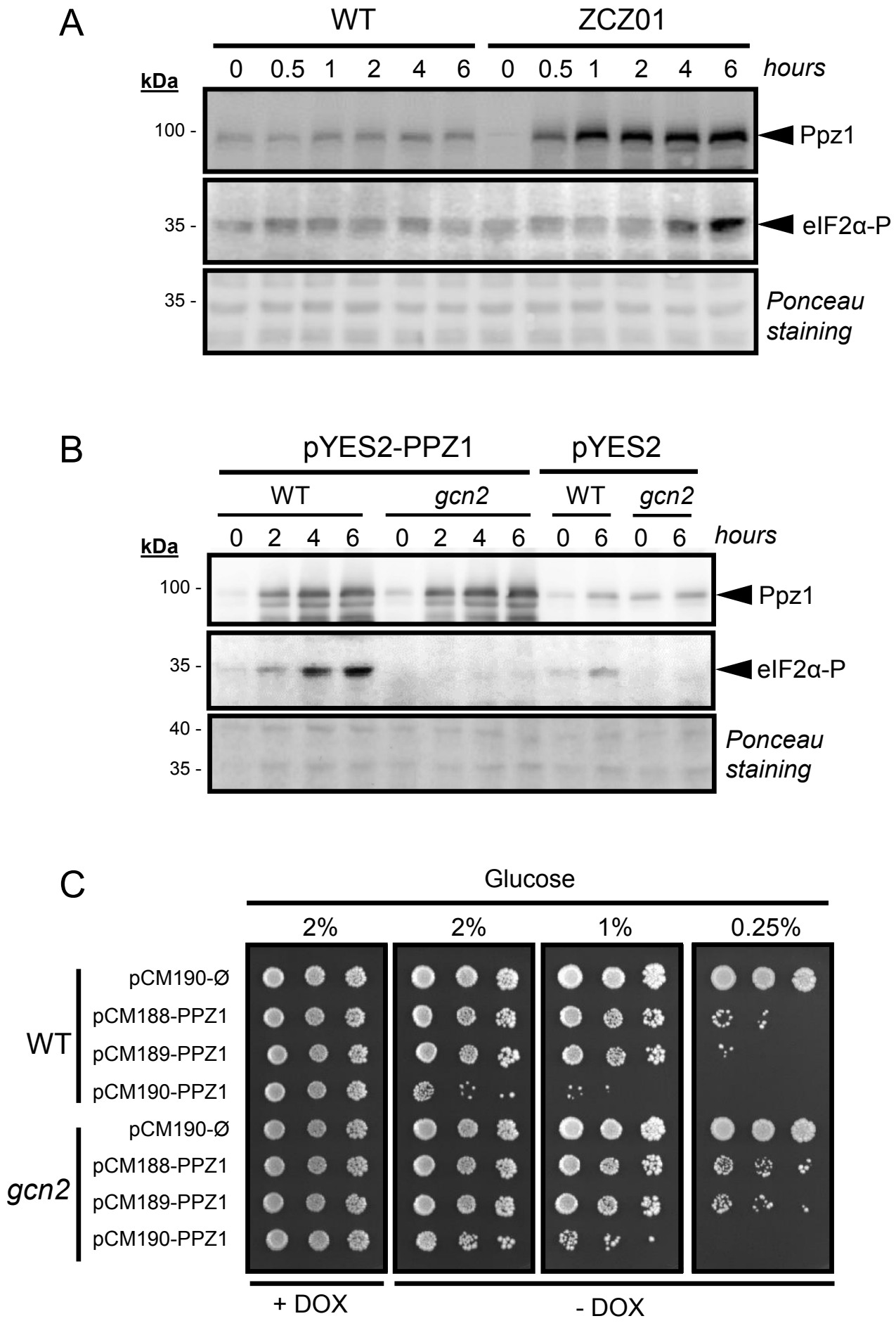
A
WT
ZCZ01
0 0.5 1 2 4 6 0 0.5 1 2 4 6 hours
kDa
100 -
Ppz1
35 -
eIF2α-P
35 -
Ponceau staining
B
pYES2-PPZ1
pYES2
WT
gcn2
WT
gcn2
0 2 4 6 0 2 4 6 0 6 0 6 hours
kDa
100 -
Ppz1
35 -
eIF2α-P
40 -
35 -
Ponceau staining
C
Glucose
2%
2%
1%
0.25%
WT
pCM190-Ø
pCM188-PPZ1
pCM189-PPZ1
pCM190-PPZ1
gcn2
pCM190-Ø
pCM188-PPZ1
pCM189-PPZ1
pCM190-PPZ1
+ DOX
- DOX

Fig. 6

Supplemental Information

Overexpression of budding yeast protein phosphatase Ppz1 impairs translation

Carlos Calafí[1,a], María López-Malo[1,a], Diego Velázquez[1], Chunyi Zhang[1], José Fernández-Fernández[2,3], Olga Rodríguez-Galán[2,3], Jesús de la Cruz[2,3], Joaquín Ariño[1,4], Antonio Casamayor[1,4,*]

[1] Institut de Biotecnologia i Biomedicina, Universitat Autònoma de Barcelona, Cerdanyola del Vallès, Catalonia, Spain.

[2] Instituto de Biomedicina de Sevilla, Hospital Universitario Virgen del Rocío/CSIC/Universidad de Sevilla, Seville, Spain.

[3] Departamento de Genética, Facultad de Biología, Universidad de Sevilla, Seville, Spain.

[4] Departament de Bioquímica i Biologia Molecular, Facultat de Veterinària, Universitat Autònoma de Barcelona, Cerdanyola del Vallès, Catalonia, Spain.

[a] These authors contributed equally to this work and are listed in alphabetical order.

* Correspondence to Antonio Casamayor, e-mail: antonio.casamayor@uab.cat

INDEX

1. Supplementary Materials and Methods

1.a Cloning into YEp195 plasmid of the positive clones obtained in the screening for multicopy suppressors.

The plasmid **YEp195-DOT6**, which contains the *DOT6* gene under the control of its own promoter, was obtained by cloning the 4.14 kb PstI/XbaI fragment from the 13.2.10 clone into the same sites of YEp195. The **YEp195-SPO20** construct contains the 3.23 kb SphI/SphI fragment from the 24.2.20 clone. **YEp195-RPS15** contains the 1.55 kb HindIII/HindIII fragment from the 24.1.43 clone. **YEp195-RPP2A** contains the 2.4 kb EcoRI/EcoRI fragment from the 24.1.43 clone. **YEp195-RPL37B** contains the 2.68 kb PstI/BamHI fragment from the 24.3.7 clone. The next genes were PCR-amplified from the specified positive clones with the detailed oligonucleotides as primers. The 2.18 kb PCR product containing the *RPS6A* gene was amplified from the 13.2.19 clone using the primers RPS6A_Fw_SalI and RPS6A_Rv_SacI and cloned into the *Sa*lI site of YEp195 to prepare the **YEp195-RPS6A** construct. The 1.59 kb PCR product containing the *SWM1* gene was amplified from the 13-2 clone using the primers SWM1_For_PstI and SWM1_Rev_SalI and cloned into the PstI/SalI sites of YEp195 to obtain the **YEp195-SWM1** plasmid. The 2.00 kb PCR product containing the *RPL37A* gene was amplified from the c2-13d-D4 clone using the primers RPL37A_For_BamHI and RPL37A_Rev_PstI and cloned into the BamHI/PstI sites of YEp195 to get the **YEp195-RPL37A** construct. **YEp195-NOC2** was obtained by cloning into the *Pst*I/*Sac*I sites of YEp195 the 3.45 kb PCR product containing the *NOC2* gene amplified from the c2-13-C-3d clone using the primers NOC2_For_PstI and NOC2_Rev_SacI. All of these inserts (except for *RPL37B)* were also cloned at the same sites in the YEp181 vector.

1.b Other plasmids prepared in this study

The plasmid **YEp195-SKY1** was constructed by cloning the 3.2 kb PCR-amplified fragment with oligonucleotides SKY1_FOR and SKY1_REV (3.2-kbp) into the *Sal*I/*Bam*HI sites of the YEp195 empty plasmid.

1.c Screening of the EUROFAN knockout collection

Pools of up to 96 single mutants from the *EUROFAN* knockout collection were transformed with plasmid pYES2-PPZ1, where *PPZ1* is under control of the galactose-inducible promoter p*GAL1-10*. The transformation was plated on synthetic medium plates lacking uracil and containing 2% of raffinose, to quantify the total number of transformants, and in plates containing 2% raffinose plus 2% galactose, where *PPZ1* expression is induced at toxic levels. Because in pilot experiments using wild-type cells transformed with pYES2-PPZ1 we observed some background growth of colonies in raffinose plus galactose plates (0.16% on the average), only transformed mutant pools showing a ratio of colonies at least 3-fold higher than the reference wild-type strain were initially considered as putative positives. A total number of 2.47 millions of clones were plated and 6 pools were identified as providing a number of growing colonies above the threshold. Genomic DNA was obtained from a representation of growing clones and subjected to PCR using the U1 and K2 oligonucleotides (Table S1) to amplify part of its disruption cassette encompassing the mutant-specific barcode (UPTAG) [1]. DNA sequencing of the barcode-containing PCR product allowed the identification of the deletion mutants. Mutant strains identified in the first round were made *de novo* (main text, Table 1), transformed with plasmid pYES2-PPZ1, and their growth re-analyzed. Ppz1 expression levels were also analyzed for these deletion mutants by western blot.

1.d GST-Ppz1^{R451L} purification

To purify GST and GST-Ppz1^{R451L}, together with the respectively pulled down proteins, frozen cells were resuspended in 150 µl of lysis buffer (50 mM Tris-HCl, pH 7.5, 150 mM NaCl, 10% Glycerol, and EDTA-free Protease Inhibitor Cocktail (Roche) supplemented with 1% Triton-X-100, 0.1% SDS and 1 mM PMSF. About 150 µl of 0.5 mm Zirconia beads (BioSpec # 11079105z) were added, cells were vortexed briefly and lysed using a FastPrep cell breaker (FastPrep 24, MP Biomedicals) at setting 5.5 for 25 seconds. This process was repeated five times, with intervals of one-minute incubation of the samples at -20°C. Finally, samples were centrifuged at 4°C at 15700xg for 15 minutes and the supernatants were incubated over-night at 4°C with 250 µL of Glutathione Sepharose 4B beads (GE

Healthcare) with mild rotation. The beads were washed 8 times with the same buffer using Multi Screen 96-well filter plates (Millipore), and then twice with the same buffer without SDS and Triton-X-100. Glutathione-beads were mixed with 4x Loading buffer (200 mM Tris-HCl, pH 6.8, 40% glycerol, 8% SDS, 0.4% bromophenol blue) plus 5 % of ß-mercaptoethanol, heated for 5 minutes at 95°C and GST bound proteins resolved by SDS-PAGE (8% of acrylamide).

1.e Mass spectrometry analysis

Samples were digested either manually or using an automatic device (DigestPro MS, Intavis), with previous reduction with dithiothreitol (DTT), derivatization by alkylation with iodoacetamide in the dark and subsequent enzymatic digestion with trypsin at 37 °C. After elution with water and acetonitrile (1:1) plus 0.2% trifluoroacetic acid the resulting peptide mixture was spotted on an MALDI plate with a α-cyano-4-hydroxycinnamic matrix and analyzed using a MALDI-TOF/TOF mass spectrometer (UltrafleXtreme Bruker). The combined TOF and TOF/TOF spectra were interpreted by database search (Mascot, Matrix Science, MA, USA). The databases used for identification were NCBI (non-redundant) and SwissProt (taxonomy *Saccharomyces cerevisiae*). Significance threshold of the MOWSE score was $p<0.05$.

2. Peptide identification by Mass Spectrometry of GST-Ppz1 and relevant interacting proteins. Residues labeled in blue correspond to peptides identified in one experiment; red residues correspond to peptides identified in two experiments and red in bold style those identified in three different experiments.

Ppz1 (AJS96320.1). Serine/threonine protein phosphatase Z.

```
  1 MGNSSSKSSK KDSHSNSSSR NPRPQVSRTE TSHSVKSAKS NKSSRSRRSL
 51 PSSSTTNTNS NVPDPSTPSK PNLEVNHQRH SSHTNRYHFP SSSHSHSNSQ
101 NELLTTPSSS STKRPSTSRR SSYNTKAAAD LPPSMIQMEP KSPILKTSNS
151 STHVSKHKSS YSSTYYENAL TDDDNDDKDN DISHTKRFSR SSNSRPSSIR
201 SGSVSRRKSD VTHEEPNNGS YSSNNQENYL VQALTRSNSH ASSLHSRKSS
251 FGSDGNTAYS TPLNSPGLSK LTDHSGEYFT SNSTSSLNHH SSRDIYPSKH
301 ISNDDDIENS SQLNDIHASM ENVNDKNNNI TDSKKDPDEE FNDIMQSSGN
351 KNAPKKFKKP IDIDETIQKL LDAGYAAKRT KNVCLKNNEI LQICIKAREI
401 FLSQPSLLEL SPPVKIVGDV HGQYGDLLRL FTKCGFPPSS NYLFLGDYVD
451 RGKQSLETIL LLFCYKIKYP ENFFLLRGNH ECANVTRVYG FYDECKRRCN
```

```
501 IKIWKTFIDT FNTLPLAAIV AGKIFCVHGG LSPVLNSMDE IRHVVRPTDV
551 PDFGLINDLL WSDPTDSPNE WEDNERGVSY CYNKVAINKF LNKFGFDLVC
601 RAHMVVEDGY EFFNDRSLVT VFSAPNYCGE FDNWGAVMSV SEGLLCSFEL
651 LDPLDSAALK QVMKKGRQER KLANQQQQMM ETSITNDNES QQ
```

Rpl3 (NP_014706.1). Ribosomal 60S subunit protein L3.

```
  1 MSHRKYEAPR HGHLGFLPRK RAASIRARVK AFPKDDRSKP VALTSFLGYK
 51 AGMTTIVRDL DRPGSKFHKR EVVEAVTVVD TPPVVVVGVV GYVETPRGLR
101 SLTTVWAEHL SDEVKRRFYK NWYKSKKKAF TKYSAKYAQD GAGIERELAR
151 IKKYASVVRV LVHTQIRKTP LAQKKAHLAE IQLNGGSISE KVDWAREHFE
201 KTVAVDSVFE QNEMIDAIAV TKGHGFEGVT HRWGTKKLPR KTHRGLRKVA
251 CIGAWHPAHV MWSVARAGQR GYHSRTSINH KIYRVGKGDD EANGATSFDR
301 TKKTITPMGG FVHYGEIKND FIMVKGCIPG NRKRIVTLRK SLYTNTSRKA
351 LEEVSLKWID TASKFGKGRF QTPAEKHAFM GTLKKDL
```

eEF1α (NP_009676.1; EF1A_YEAST). Translation elongation factor EF-1α. Product of *TEF1* or *TEF2* genes.

```
  1 MGKEKSHINV VVIGHVDSGK STTTGHLIYK CGGIDKRTIE KFEKEAAELG
 51 KGSFKYAWVL DKLKAERERG ITIDIALWKF ETPKYQVTVI DAPGHRDFIK
101 NMITGTSQAD CAILIIAGGV GEFEAGISKD GQTREHALLA FTLGVRQLIV
151 AVNKMDSVKW DESRFQEIVK ETSNFIKKVG YNPKTVPFVP ISGWNGDNMI
201 EATTNAPWYK GWEKETKAGV VKGKTLLEAI DAIEQPSRPT DKPLRLPLQD
251 VYKIGGIGTV PVGRVETGVI KPGMVVTFAP AGVTTEVKSV EMHHEQLEQG
301 VPGDNVGFNV KNVSVKEIRR GNVCGDAKND PPKGCASFNA TVIVLNHPGQ
351 ISAGYSPVLD CHTAHIACRF DELLEKNDRR SGKKLEDHPK FLKSGDAALV
401 KFVPSKPMCV EAFSEYPPLG RFAVRDMRQT VAVGVIKSVD KTEKAAKVTK
451 AAQKAAKK
```

Rpl4a (P02994; EF1A_YEAST). Ribosomal 60S subunit protein L4A and L4B (most peptides could be from the product of the *RPL4B* gene).

```
  1 MSRPQVTVHS LTGEATANAL PLPAVFSAPI RPDIVHTVFT SVNKNKRQAY
 51 AVSEKAGHQT SAESWGTGRA VARIPRVGGG GTGRSGQGAF GNMCRGGRMF
101 APTKTWRKWN VKVNHNEKRY ATASAIAATA VASLVLARGH RVEKIPEIPL
151 VVSTDLESIQ KTKEAVAALK AVGAHSDLLK VLKSKKLRAG KGKYRNRRWT
201 QRRGPLVVYA EDNGIVKALR NVPGVETANV ASLNLLQLAP GAHLGRFVIW
251 TEAAFTKLDQ VWGSETVASS KVGYTLPSHI ISTSDVTRII NSSEIQSAIR
301 PAGQATQKRT HVLKKNPLKN KQVLLRLNPY AKVFAAEKLG SKKAEKTGTK
351 PAAVFTETLK HD
```

Rpl2b (NP_012246.1). Ribosomal 60S subunit protein L2A and L2B. Product of *RPL2B* gene. Identical to Rpl2a, product of the *RPL2A* gene.

```
  1 MGRVIRNQRK GAGSIFTSHT RLRQGAAKLR TLDYAERHGY IRGIVKQIVH
 51 DSGRGAPLAK VVFRDPYKYR LREEIFIANE GVHTGQFIYA GKKASLNVGN
101 VLPLGSVPEG TIVSNVEEKP GDRGALARAS GNYVIIIGHN PDENKTRVRL
151 PSGAKKVISS DARGVIGVIA GGGRVDKPLL KAGRAFHKYR LKRNSWPKTR
201 GVAMNPVDHP HGGGNHQHIG KASTISRGAV SGQKAGLIAA RRTGLLRGSQ
251 KTQD
```

Rpl13b (NP_013862.1). Ribosomal 60S subunit protein L13B. Product of *RPL13B* gene (most peptides could be from the product of the *RPL13A* gene). Distinctive residues are shown in grey background.

```
  1 MAISKNLPIL KNHFRKHWQE RVKVHFDQAG KKVSRRNARA ARAAKIAPRP
 51 LDLLRPVVRA PTVKYNRKVR AGRGFTLAEV KAAGLTAAYA RTIGIAVDHR
101 RQNRNQEIFD ANVQRLKEYQ SKIIVFPRDG KAPEAEQVLS AAATFPIAQP
151 ATDVEARAVQ DNGESAFRTL RLARSEKKFR GIREKRAREK AEAEAEKKK
```

Rpl10 (NP_013862.1). Ribosomal 60S subunit protein L10. Product of *RPL10* gene.

```
  1 MARRPARCYR YQKNKPYPKS RYNRAVPDSK IRIYDLGKKK ATVDEFPLCV
 51 HLVSNELEQL SSEALEAARI CANKYMTTVS GRDAFHLRVR VHPFHVLRIN
101 KMLSCAGADR LQQGMRGAWG KPHGLAARVD IGQIIFSVRT KDSNKDVVVE
151 GLRRARYKFP GQQKIILSKK WGFTNLDRPE YLKKREAGEV KDDGAFVKFL
201 SKKGSLENNI REFPEYFAAQ A
```

Glutathione S-transferase of *Schistosoma Japonicum* (1GNE_A)

```
  1 SPILGYWKIK GLVQPTRLLL EYLEEKYEEH LYERDEGDKW RNKKFELGLE
 51 FPNLPYYIDG DVKLTQSMAI IRYIADKHNM LGGCPKERAE ISMLEGAVLD
101 IRYGVSRIAY SKDFETLKVD FLSKLPEMLK MFEDRLCHKT YLNGDHVTHP
151 DFMLYDALDV VLYMDPMCLD AFPKLVCFKK RIEAIPQIDK YLKSSKYIAW
201 PLQGWQATFG GGDHPPKSDL VPRGSMELDK WA
```

TABLE S1. OLIGONUCLEOTIDES USED FOR PLASMID OR STRAIN CONSTRUCTION.

Name	Sequence (5'-3')
OMLM1	TCATCGTTATAGTCGCTTCTTTTCCCCTAGAGGCTTTGT CCAGCTGAAGCTTCGTACGC
OMLM2	TCCTTTTTCGAAGATTTTGAACTTGAATTACCCATTTTG AAAATAGGCCACTAGTGGATCTG
OMLM3	CGGGATCCAAAATGGGTAATTCAAGTTCAAAATC
OMLM4	TGCACTGCAGTTACTGTTGAGATTCGTTATCATTTG
OMLM5	AGTCGCTTCTTTTCCCCTAG
OMLM6	CTTTGATGGAGTGGAGGG
U1	GATGTCCACGAGGTCTCT
K2	CACGTCAAGACTGTCAAGGA
SKY1_FOR	ACGCGTCGACCTACCAAATGACCCAGGGA
SKY1_REV	CGGGATCCATCATCCTTCACCAGGACAA
PPZ1_F4	TCATCGTTATAGTCGCTTCTTTTCCCCTAGAGGCTTTGT CGAATTCGAGCTCGTTTAAAC
PPZ1_R2	TTTCGAAGATTTTGAACTTGAATTACCCATTTTGAGATC CGGGTTTT
E1_kpnI	CGGGTACCATGTTCAGATAGCTGCC
K3	GTTAAGTGCGCAGAAAGTAA
GAL4 FW	CGGAGATGACTGCCAGGTGC
GAL4 REV	TGTCCGAATGGAGGGGCTCAG
GAL11 FW	GAAGCGGCGAGGCAGCC
GAL11 REV	GTTACTGGTGACACCGATGC
MED2 FW	GCAGTGTGTGTACGATACCT
MED2 REV	ATAGTGGATGTACTGCTGCTG
PGD1 FW	CTGTACCTGGACTCGCAGGC
PGD1 REV	TAGCACCAGCCTTGGCAGC
RPS6A_Fw_SalI	CACGTCGACTCGAACAATCAGTCCAACTCAAG
RPS6A_Rv_SacI	CGAGCTCGCTTGGATATTCAGTTGAGG
SWM1_For_PstI	ACACTGCAGTCTAGTCTCAACGGCTG
SWM1_Rev_SalI	TTGGTCGACCATCATCATTATG
RPL37A_For_BamHI	ACGGATCCACTGTCCTGTAGGG
RPL37A_Rev_PstI	GACCTGCAGCTTTCCGGC
NOC2_For_PstI	GCACTGCAGCCTCTGGGGACGTAGTTC
NOC2_Rev_SacI	CGAGCTCTAGAGATGGTGGTCTGAGG
BamHI_Npl3_prom_Fw	AGCGGATCCTCTCAGCTCCGGAACCGGTA
SacI_Npl3_term_Rev	AGCGAGCTCTCCTGCCCGTATGTTGAAGA

TABLE S2. PLASMIDS USED IN THIS STUDY PREVIOUSLY DESCRIBED.

Name	Description	Source
YEp195-HAL3	*SIS2/HAL3* under the control of its own promoter.	[2]
pRS699-HsHal3	Hal3 homolog from *Homo sapiens* (HsCoaC) under the control of the *PMA1* promoter.	[3]
YEp195-VHS3	*VHS3* under the control of its own promoter.	[4]
pRS315 -RFP-NOP1-RPL25-GFP	Large ribosomal subunit export reporter.	[5]
pRS315-RFP-NOP1-RPS3-GFP	Small ribosomal subunit export reporter.	[5]
pYES2-PPZ1	*PPZ1* ORF under the control of *GAL1-10* promoter.	[6]
pEGH-PPZ1	*PPZ1* ORF fused in its N-terminus to GST under the control of *GAL1-10* promoter.	[7]
pFA6a-kanMX6-pGAL1	Source for the kanMX6-pGAL1 cassette.	[8]
pCM188	Centromeric, $tetO_2$ promoter.	[9]
pCM189	Centromeric, $tetO_7$ promoter.	[9]
pCM190	Episomal, $tetO_7$ promoter.	[9]

TABLE S3. OLIGONUCLEOTIDES USED AS PROBES FOR MONITORING rRNA MATURATION.

Name	Sequence (5'-3')
Probe b (18S)	CATGGCTTAATCTTTGAGAC
Probe c (3-D/A_2)	GACTCTCCATCTCTTGTCTTCTTG
Probe d (A_2/A_3)	TGTTACCTCTGGGCCC
Probe e (5.8S)	TTTCGCTGCGTTCTTCATC
Probe f (E/C_2)	GGCCAGCAATTTCAAGTTA
Probe g (C_1/C_2)	GAACATTGTTCGCCTAGA
Probe h (25S)	CTCCGCTTATTGATATGC
Probe 5S	GGTCACCCACTACACTACTCGG

TABLE S4. GROWTH SCORES IN SYNTHETIC MEDIUM CONTAINING 0.25% GLUCOSE AS CARBON SOURCE OF CELLS OVEREXPRESSING COMBINATIONS OF TWO SUPPRESSOR GENES.

Ranking from 0 (no detected growth) to 5 (growth of strain MLM04 overexpressing Hal3)

		YEp181								
YEp195		Ø	*HAL3*	*DOT6*	*RPS6A*	*SPO20*	*RPS15*	*SWM1*	*RPP2A*	*RPL37A*
	Ø	0								
	HAL3	5								
	DOT6	2	4.5							
	RPS6A	3	4.5	3						
	SPO20	4	4.5	4	4.5					
	RPS15	3	4.5	3	3.5	4.5				
	SWM1	3	4.5	4	4	4	3			
	RPP2A	3.5	4.5	4	4	3.5	4	4		
	RPL37A	3	5	3	3	4.5	3.5	4	3.5	
	NOC2	4	5	4	4	4	4	4	4	4

TABLE S5. GROWTH SCORES IN SYNTHETIC MEDIUM CONTAINING 2% GALACTOSE AS CARBON SOURCE OF CELLS OVEREXPRESSING COMBINATIONS OF TWO SUPPRESSOR GENES.

Ranking from 0 (no detected growth) to 5 (growth of strain MLM04 overexpressing Hal3)

		YEp181								
YEp195		Ø	*HAL3*	*DOT6*	*RPS6A*	*SPO20*	*RPS15*	*SWM1*	*RPP2A*	*RPL37A*
	Ø	0								
	HAL3	5								
	DOT6	0	5							
	RPS6A	0	5	0						
	SPO20	0	5	1	4.5					
	RPS15	0	5	0	0	2				
	SWM1	0	4.5	2.5	2.5	0	0			
	RPP2A	0	5	0	0	0	0	0		
	RPL37A	0	5	0	0	4	0	0	0	
	NOC2	2	5	2	3	3.5	2	3.5	2.5	2.5

TABLE S6. DETECTED PROTEINS PULLED-DOWN WITH GST AND GST-Ppz1^{R451L}.

Databases used for analysis: NCBI nr (**NC**) and SwissProt 2020_01 Taxonomy: *S. cerevisiae* (**SP**). Mascot scores greater than 50 for searches in SP, or greater than 92 for searches in NC, were considered significant (p<0.05). Slice: identification of gel slices shown in Fig. 5A. Superscripts (2), (3) indicate proteins identified in 2 or 3 independent experiments, respectively. Proteins identified as first hit in at least one experiment are denoted with "§". Matched: number of peptides matching with the protein. % Coverage: Protein sequence coverage. The range of coverage for proteins identified in more than one experiment and the overall coverage (in parentheses) are shown. Protein names in bold denote proteins involved in the translation process.

Pull-down GST-Ppz1								Pull-down GST						
Slice	Protein ID	MW (kD)	Mascot Score	Expect	Matched	% Coverage	Database	Protein ID	MW (kD)	Mascot Score	Expect	Matched	% Coverage	Database
I	Ppz1^{2,§}	78	300	7.9E-27	36	48-53 (62)	SP	Few signals detected with low intensity						
	GST	27	77	2	13	46	NC							
II	Ssa1§	70	133	4.0E-10	19	28	SP	Ssa1§	70	97	1.6E-06	15	22	SP
	Ssa2	70	86	2.1E-05	16	28	SP	Ssa2	70	85	2.3E-05	14	21	SP
								Ptc6	50	59	0.011	9	21	SP
III	**Rpl3**§	44	185	2.9E-11	22	54	NC	Eno2 and Pgk1 signals with low intensities.						
	EF-1α^{3,§}	50	128	1.5E-05	18	32-38 (53)	NC							
	Eno2§	47	110	7.9E-08	21	47	SP							
	Pgk1	45	104	3.1E-07	19	50	SP							
	Eno1	47	93	4.3E-06	17	41	SP							
IV	Fba1§	40	113	4.0E-08	13	34	SP	Fba1 signal with low intensity						
	Rpl4A/B	39	81	6.4E-05	11	40	SP							
V	**Rpl2B^{2,§}**	27	126	2.3E-05	11	60-65 (67)	NC	No relevant signal detected						
VI	Ura3§	29	142	5.0E-11	21	71	SP	Ura3	29	63	3.8E-03	12	42	SP
	Rpl13B§	23	123	4.7E-05	12	54	NC							
	Gpm1	28	114	3.1E-08	19	53	SP							
	Rpl10	25	89	1.6E-04	10	51	NC							
								GST*,§	26	198	8.9E-15	26	67	SP

REFERENCES

[1] D.E. Kelly, D.C. Lamb, S.L. Kelly, Genome-Wide Generation of Yeast Gene Deletion Strains, Comp. Funct. Genomics. 2 (2001) 236–242. https://doi.org/10.1002/cfg.95.

[2] E. de Nadal, J. Clotet, F. Posas, R. Serrano, N. Gomez, J. Ariño, The yeast halotolerance determinant Hal3p is an inhibitory subunit of the Ppz1p Ser/Thr protein phosphatase., Proc. Natl. Acad. Sci. U. S. A. 95 (1998) 7357–62. https://doi.org/0.1073/pnas.95.13.7357.

[3] A. Ruiz, A. Gonzalez, I. Munoz, R. Serrano, J.A. Abrie, E. Strauss, J. Arino, Moonlighting proteins Hal3 and Vhs3 form a heteromeric PPCDC with Ykl088w in yeast CoA biosynthesis, Nat. Chem. Biol. 5 (2009) 920–928. https://doi.org/10.1038/nchembio.243.

[4] A. Ruiz, I. Muñoz, R. Serrano, A. Gonzalez, E. Simon, J. Arino, Functional characterization of the Saccharomyces cerevisiae VHS3 gene: a regulatory subunit of the Ppz1 protein phosphatase with novel, phosphatase-unrelated functions, J. Biol. Chem. 279 (2004) 34421–34430. https://doi.org/10.1074/jbc.M400572200.

[5] C. Ulbrich, M. Diepholz, J. Bassler, D. Kressler, B. Pertschy, K. Galani, B. Böttcher, E. Hurt, Mechanochemical removal of ribosome biogenesis factors from nascent 60S ribosomal subunits., Cell. 138 (2009) 911–22. https://doi.org/10.1016/j.cell.2009.06.045.

[6] J. Clotet, F. Posas, E. De Nadal, J. Arino, The NH2-terminal extension of protein phosphatase PPZ1 has an essential functional role, J. Biol. Chem. 271 (1996) 26349–26355. https://doi.org/10.1074/jbc.271.42.26349.

[7] H. Zhu, Global Analysis of Protein Activities Using Proteome Chips, Science (80-.). 293 (2001) 2101–2105. https://doi.org/10.1126/science.1062191.

[8] M.S. Longtine, A. Mckenzie III, D.J. Demarini, N.G. Shah, A. Wach, A. Brachat, P. Philippsen, J.R. Pringle, Additional modules for versatile and economical PCR-based gene deletion and modification in Saccharomyces cerevisiae, Yeast. 14 (1998) 953–961. https://doi.org/10.1002/(SICI)1097-0061(199807)14:10<953::AID-YEA293>3.0.CO;2-U.

[9] E. Garí, L. Piedrafita, M. Aldea, E. Herrero, A set of vectors with a tetracycline-regulatable promoter system for modulated gene expression in Saccharomyces cerevisiae., Yeast. 13 (1997) 837–48. https://doi.org/10.1002/(SICI)1097-0061(199707)13:9<837::AID-YEA145>3.0.CO;2-T.

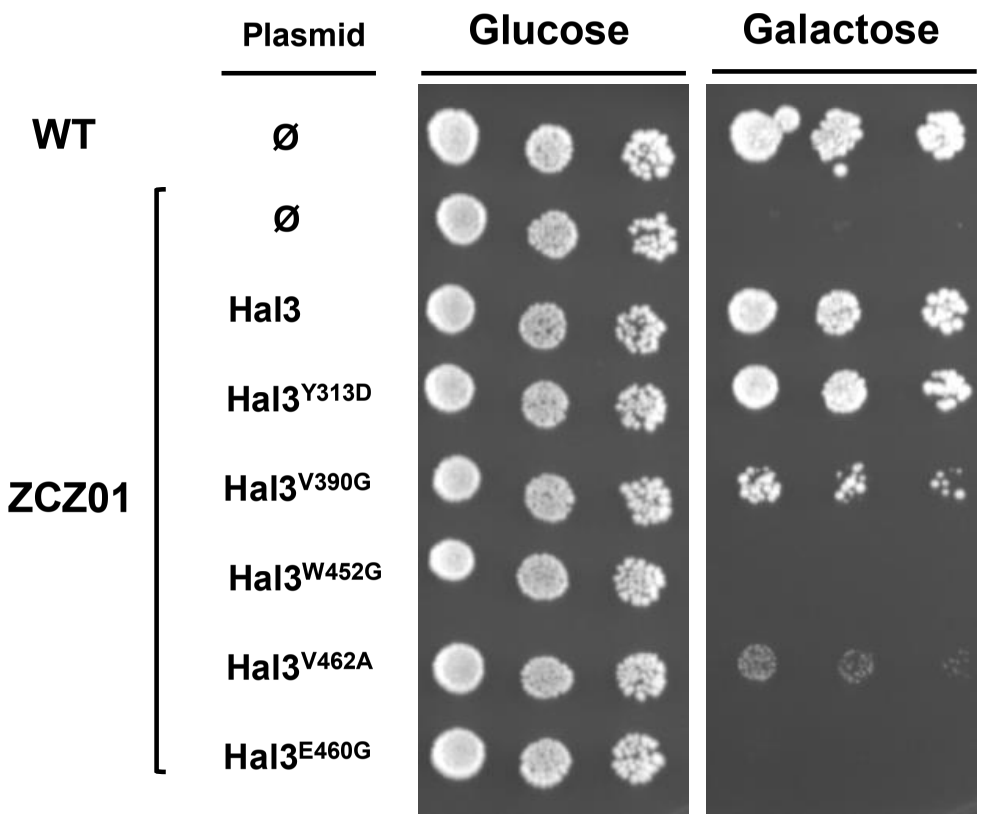

	Ability to inhibit PPase	Ability to bind Ppz1
WT	*****	*****
ZCZ01 Ø	*****	****
ZCZ01 Hal3	****	*
ZCZ01 $Hal3^{Y313D}$	***	**
ZCZ01 $Hal3^{V390G}$	**	****
ZCZ01 $Hal3^{W452G}$	*	***
ZCZ01 $Hal3^{V462A}$		
ZCZ01 $Hal3^{E460G}$		

Suppressor effect of different mutated versions of Hal3 on Ppz1 toxicity. The indicated versions of Hal3 were introduced as high-copy (YEplac195-based) plasmids in strain ZCZ01. Cultures were spotted at OD_{600} = 0.05 and at 1/5 dilutions on synthetic medium lacking uracil and using glucose or galactose as carbon source. Growth was recorded after 4 days. The relative abilities of the different Hal3 versions to bind to and inhibit Ppz1, as determined in Muñoz *et al.* 2004 (PMID:15292171), are indicated (*****, WT; *, virtually lost).

Fig. S1

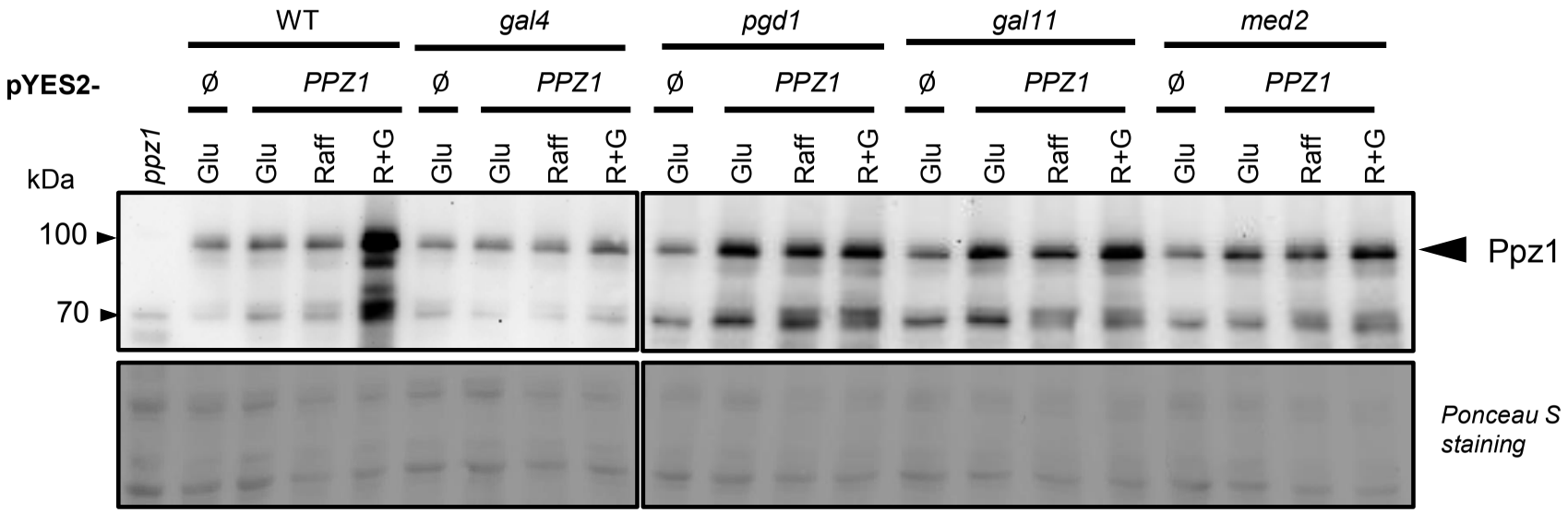

Determination of the Ppz1 levels in wild-type (WT) and in the indicated mutant strains found in our deletion mutant screen. Overnight cultures were diluted to OD_{600} 0.2 and incubated at 28ºC in a glucose- (Glu) or raffinose-containing (Raff) medium. In case of Raff+Gal (R+G), after 4 hours cultures were induced by adding 2% galactose. Samples were taken 2 hours post-induction (6 hours post-inoculation in the non-induced cultures) and Ppz1 present in cell extracts was immunodetected. Ponceau S staining is shown as loading control.

Fig. S2

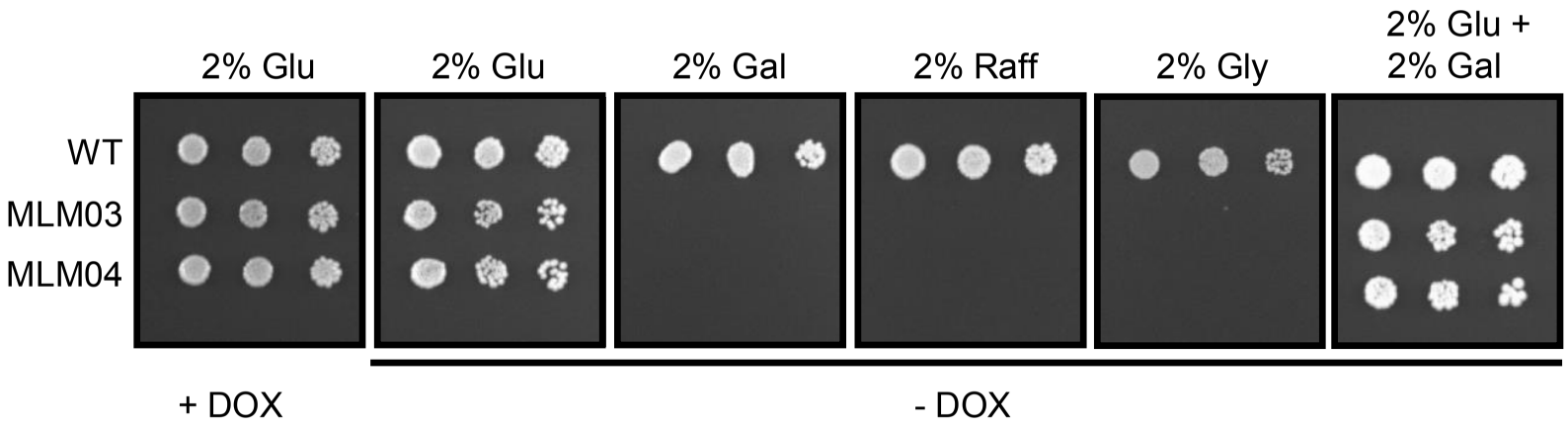

Effect of different carbon sources on cell growth in cells over-expressing Ppz1. Cultures of wild-type (WT), MLM03 and MLM04 yeast strains grown in the absence of doxycycline (-DOX) were spotted at OD_{600} = 0.05 and at 1/5 dilutions on YP medium using containing the indicated carbon sources. Same strains cultured in the presence of doxycycline (+DOX) were used as a positive control. Growth was recorded after 3 days.

Fig. S3

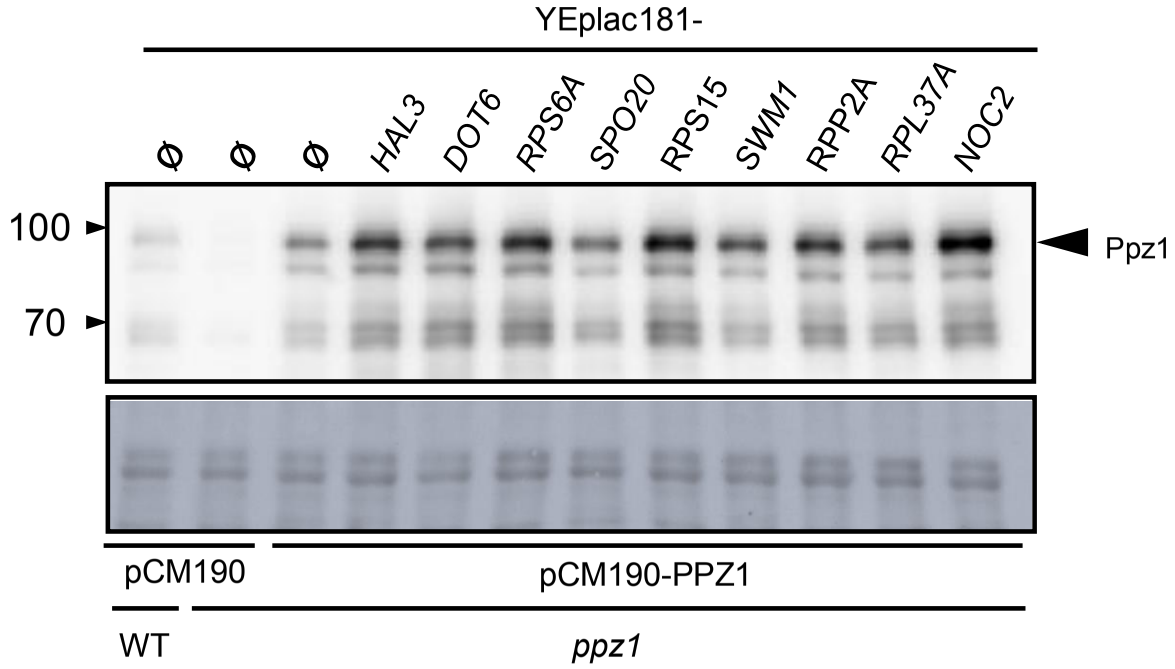

Determination of Ppz1 levels in wild-type (WT) and *ppz1* mutant cells expressing Ppz1 and the high-copy number suppressors found in our screen. Cultures of BY4741 cells containing the empty pCM190 vector (as a control) or pCM190-PPZ1 were grown to saturation in the presence of doxycycline, and diluted at OD_{600}=0.2 in synthetic medium lacking uracil in the absence of doxycycline. Cells were cultivated for 6 h at 28ºC in the absence of doxycycline to induce *PPZ1* expression. Ppz1 present in cell extracts was immunodetected. Ponceau S staining (lower panel) is shown as loading control.

Fig. S4

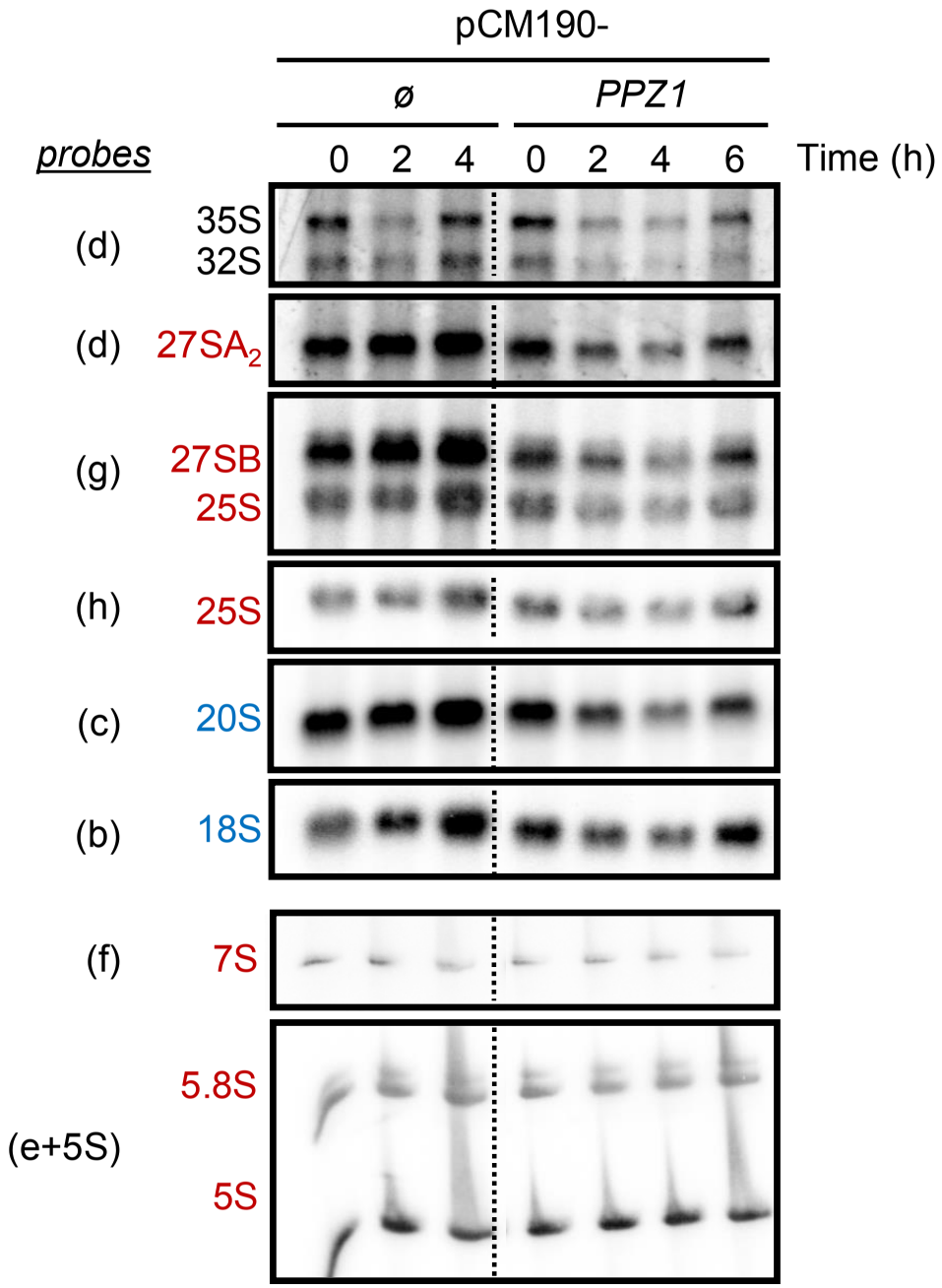

Northern blots to detect the maturation steps of the indicated rRNAs. Fresh cultures of BY4741 cells containing the empty pCM190 vector (as a control) or pCM190-PPZ1 were prepared at OD_{600} 0.2 in medium lacking uracil in the absence of doxycycline from saturated cultures previously grown in the absence of doxycycline for 8.5h. Cells were harvested at the indicated time-points, total RNA was extracted from each sample and equal amounts (5 µg) of RNA were subjected to northern hybridization. The indicated pre-rRNAs were detected using the different probes indicated on the left (between parentheses; see Table S3). Red labels indicate maturation of rRNA involved in the 60S pathway while blue labels denote the rRNAs of the 40S pathway. Dotted separate distant lanes from the same gel.

Fig. S5

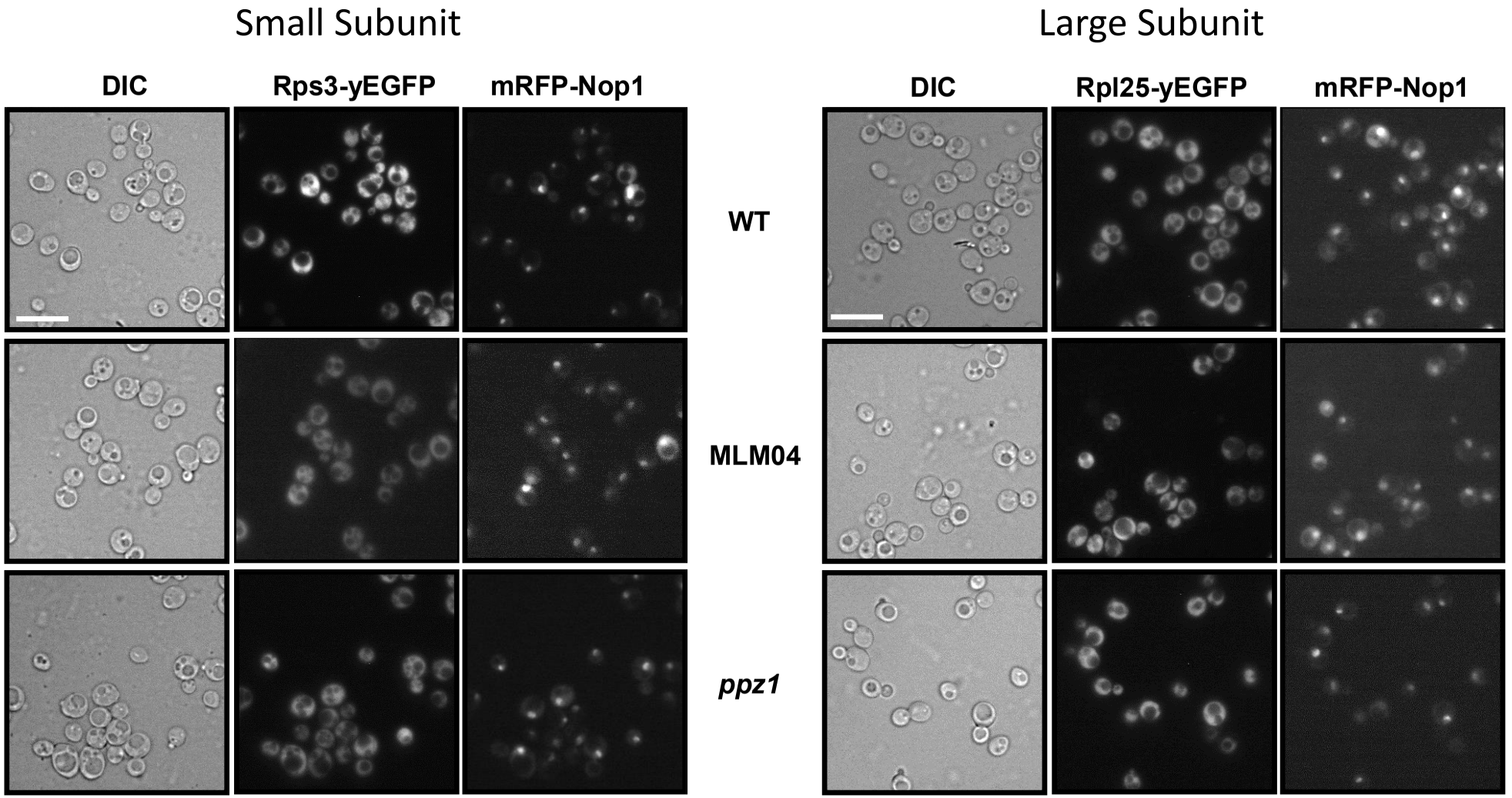

Trafficking of ribosomal proteins under overexpression of Ppz1. Saturated cultures of wild-type (WT), MLM04 and *ppz1* strains transformed with the plasmids carrying the indicated reporters were grown in medium lacking leucine in the presence of doxycycline and used to prepare fresh cultures at OD_{600}=0.2 in synthetic medium without the antibiotic. After 24 h of growth new fresh cultures were prepared in the same medium also at OD_{600}=0.2 in the absence of doxycycline, and samples were taken after 4h (in log phase) for fluorescent microscopy. Rps3-yEGFP shows localization of the small ribosome subunit, Rpl25-yEGFP the large subunit and mRFP-Nop1 labels the nucleolus. Scale bar: 10 μm.

Fig. S6

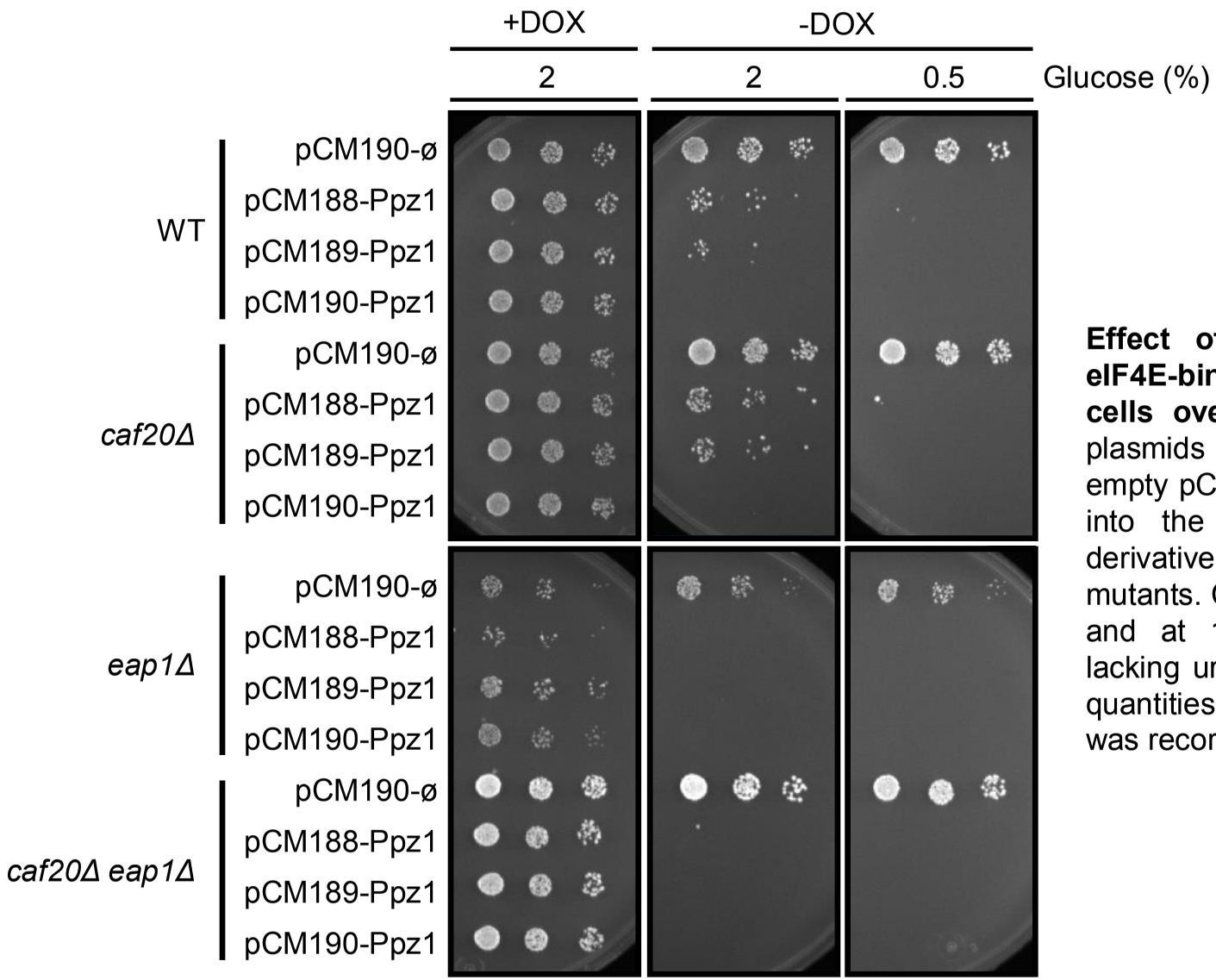

Effect of deletion of genes coding for eIF4E-binding proteins on cell growth of cells over-expressing *PPZ1*. The indicated plasmids for over-expression of Ppz1 (or the empty pCM190 as a control) were transformed into the BY4742 strain (WT) and in its derivatives *caf20Δ*, *eap1Δ* and *caf20Δ eap1Δ* mutants. Cultures were spotted at OD_{600} = 0.05 and at 1/5 dilutions on synthetic medium lacking uracil supplemented with the indicated quantities of glucose as carbon source. Growth was recorded after 3 days.

Fig. S7

CRediT author statement

Carlos Calafí: Investigation, Formal analysis, Visualization **María López-Malo**: Investigation, Formal analysis, Visualization **Diego Velázquez**: Investigation **Chunyi Zhang**: Investigation **José Fernández-Fernández**: Investigation **Olga Rodríguez-Galán**: Investigation **Jesús de la Cruz**: Conceptualization, Writing - Review & Editing, Funding acquisition **Joaquín Ariño**: Conceptualization, Formal analysis, Visualization, Writing - Original Draft, Writing - Review & Editing, Funding acquisition **Antonio Casamayor**: Conceptualization, Formal analysis, Visualization, Writing - Original Draft, Writing - Review & Editing, Funding acquisition.